

Numerical solution of the scattering problem for acoustic waves by a two-sided crack in 2-dimensional space

P.A. Krutitskii J.J. Liu* M. Sini

Keldysh Institute of Applied Mathematics, Miusskaya Sq. 4,
Moscow, 125047, Russia. email: krutitsk@math.phys.msu.su

Department of Mathematics, Southeast University
Nanjing, 210096, P.R.China. email: jjliu@seu.edu.cn

RICAM, Austrian Academy of Science
Linz, A-4040, Austria. email: mourad.sini@oeaw.ac.at

May 18, 2009

Abstract

The wave scattering problem by a crack Γ in \mathbb{R}^2 with impedance type boundary is considered. This problem models the diffraction of waves by thin two-sided cylindrical screens. A numerical method for solving the problem is developed. The solution of the problem is represented in the form of the combined angular potential and single-layer potential. The linear integral equations satisfied by the density functions are derived for general parameterized arcs. The weakly singular integrals and the Cauchy singular integral arising in these equations are computed using a highly accurate scheme with a truncation error analysis. The advantage of the scheme proposed in this paper is, in one hand, the fact that we do not need the analytic property of the crack and we allow different complex valued surface impedances in both sides of the crack. In the other hand, we avoid the hyper-singular integrals. Numerical implementations showing the validity of the scheme are presented.

Key words. Wave scattering, impedance boundary, integral equations, singularity analysis, numerics.

AMS subject classifications. 35P25, 35R30, 78A45.

1 Introduction

The scattering problems for acoustic waves in \mathbb{R}^m ($m = 2, 3$) are of great importance. Mathematically, such problems are governed by the Helmholtz equations in \mathbb{R}^m with boundary

*Correspondence author, email: jjliu@seu.edu.cn (J.J.Liu)

value specified on the boundary of the scatterer and the radiation condition at infinity for scattered wave. In case the scatterer D is a body with a closed smooth surface, these scattering problems have been extensively studied using the potential methods ([2, 4, 19, 22, 26]), the scattering problem for multiple obstacle is also considered in ([25]). In these cases, the combined single- and double-layer potential schemes ([2, 4, 22]) are proposed to express the scattered wave as well as its far-field pattern by density functions, which satisfies an integral equation derived from the boundary condition in ∂D . However, to guarantee the solvability for the density functions in the combined single- and double-layer potential scheme, the hyper-singular integrals need to be computed numerically for ∂D with Neumann or Robin boundary condition ([1, 17, 18]).

To describe the diffraction of waves by thin two-side cylindrical screens, the scattering problems of Helmholtz equation by a crack Γ (or, an open arc) in \mathbb{R}^2 are considered recently. In this case, the boundary condition on the arc should be specified, while the acoustic property of the arc in both sides may be different. For arc scattering problems, the scattered wave is continuous at the tips, but its gradient has weak power singularity. Consequently, the potential functions introduced for solving the scattering problems are not periodic nor smooth in the closure of Γ any more. Hence, compared with the scattering problems of obstacles with closed smooth boundary, these crack scattering problems are more complicated due to the eventual different surface impedances on both sides as well as the presence of the tips of crack. The inverse scattering problems for arc with Dirichlet or Neumann data on the arc has been considered in [8, 11, 12, 16, 24, 27, 28]. Physically, this means that the arc is sound-soft or sound hard. For the Laplace equation in \mathbb{R}^2 with a cut inside the domain, the Cauchy problem is also considered in [3], where both the Dirichlet and the Neumann condition are posed in both sides of the cut in the iteration process.

Let us emphasize that the impedance condition specified on the obstacle boundary is of great importance in the applied area ([5]). The introduction of surface impedance specified on the boundary has a big influence on the scattered wave. For example, an inverse scattering problem for an impenetrable obstacle with smooth surface has been studied in [20, 21], where the impedance coefficients on the boundary are found to have a strong influence on the scattering process. This is related to the so-called coating effect which, in few words, means that these coefficients can increase or decrease the amount of scattering. In [15], an inverse scattering problem for an arc with different impedance coefficients at two sides of the arc is studied, where the direct scattering process is simulated by the combined single- and double-layer potential method.

In this paper, we develop a numerical method for the direct scattering problem of a two-sided impedance arc $\Gamma \in \mathbb{R}^2$. By two-sided arc, we mean that the acoustic property of the arc in two sides may be different. If we specify two sides of Γ by Γ^+ and Γ^- , then the boundary impedance coefficient as well as the boundary data in Γ^+ and Γ^- may be different. The numerical method developed in the present paper is based on the boundary integral equation approach proposed in [9], where the integral representation for a solution of the problem is obtained in the form of a sum of a single layer potential and an angular potential.

In the case of an arc with the same impedance condition on both sides, the computational scheme has been given in [6, 7], where the analytic property of the arc and the hyper-singular integral are required.

The purpose of this paper is to give an efficient realization scheme for computing the scattered wave caused by a two-sided complex arc, using the combined angular- and single-layer potential method. Although the integral equation for the density functions has been derived in [9] and its solvability is proven there, the efficient numerical realization of this scheme is still open. More precisely, the integral system consists of a Cauchy singular integral equation of the 1st kind with additional integral condition and an integral equation of the 2nd kind with smooth kernels. Since the Cauchy singular operator has additional weak singularities at the ends, then we need to be more careful about the method of computation. On the other hand, the arc Γ is represented in [9, 10, 11] using the arc length for the parametrization, which is the restriction on this scheme. The novelty of our paper is the new numerical method for computing the integrals with high accuracy and therefore solving this very complicated system of integral equations efficiently. We produce different number of unknowns in algebraic equations for different densities in potentials, since we need to use discrete vortices for Cauchy singular integral and to take into account another additional integral condition. The problem solved in the paper has not been treated before numerically, while the problem studied numerically in [6, 7] is a particular case of our problem. One of our motivations to analyze this numerical scheme is to generate synthetic far fields needed in the corresponding inverse problem for the detection of complex cracks from far field data, see [14]. We also note that, in considering the direct scattering process in [15], the Maus's identity is applied to milder the hypersingularity caused from the double-layer potential and the impedance boundary condition of the cut, while the angular layer potential in our paper is applied directly to express the scattered wave and therefore avoid the hypersingularity in the integral equations.

This paper is organized as follows. In section 2, we state the potential method for expressing the scattered wave using the combined angular and single-layer potential method. The modification required for the crack representation with general parametrization is given. Then we derive the discrete system for these integral equations in section 3, with careful truncation error estimates for all the integral terms. This forms the basis for the error estimate of the convergence order for the scattered wave computation. In section 4, we derive the discrete system for computing the scattered wave as well as its far-field pattern using the density functions and give some numerical results. The numerical performance shows that the computing scheme is of a stable convergence order.

2 Statement of the problem and preliminary results

For given arc $\Gamma := \{x := (x_1(s), x_2(s)), s \in [a, b]\} \in \mathbb{R}^2$, we define its two sides by the following way. When the parameter s increases, the side Γ^+ is in the left-hand of Γ , and the other side, correspondingly, is denoted by Γ^- . The normal unit vector n on Γ , it is

always directed into the side Γ^- , see Figure 1 for the configuration. That is, when $n(x)$ is rotated anticlockwise through an angle $\pi/2$, it coincides with $\nu(x)$, the tangent direction of Γ is directed into the direction of s increasing. Obviously, it follows for $x(s) \in \Gamma$ that the unit normal direction is given by $n(x(s)) = \frac{(\dot{x}_2(s), -\dot{x}_1(s))}{|\dot{x}(s)|} = \frac{\dot{x}(s)^\perp}{|\dot{x}(s)|}$, where $|\dot{x}(s)| := \sqrt{\dot{x}_1(s)^2 + \dot{x}_2(s)^2}$, $\dot{f}(s) := f'(s)$ means the derivative with respect to variable s . Moreover, we assume that Γ is smooth enough such as $\Gamma \in C^{2,\lambda}$, $\lambda \in (0, 1]$, but the analytic smoothness is not necessary.

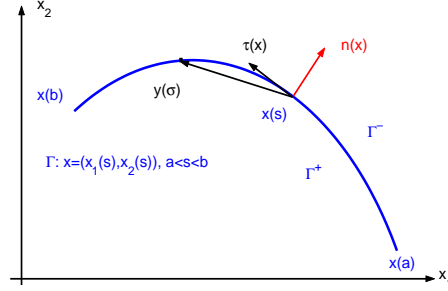


Figure 1: Geometric configuration of an arc

For given incident plane wave $u^i(x) = e^{ikx \cdot d}$ with wave number $k > 0$ and incident direction d , consider the following scattering problem for total wave $v(x) = u^i(x) + u^s(x)$ by arc Γ :

$$\begin{cases} \Delta v + k^2 v = 0, & \mathbb{R}^2 \setminus \Gamma \\ \frac{\partial v}{\partial n} - ik\sigma^+ v = 0, & \Gamma^+ \\ \frac{\partial v}{\partial n} + ik\sigma^- v = 0, & \Gamma^- \\ \frac{\partial u^s}{\partial |x|} - ik u^s(x) = o\left(\frac{1}{\sqrt{|x|}}\right), & |x| \rightarrow \infty \end{cases} \quad (2.1)$$

The boundary condition on Γ^\pm means that the acoustic property of arc in the two sides is different, where the impedance functions σ_\pm are smooth satisfying $\Re\sigma^\pm > \sigma_0 > 0$ in Γ .

Noticing that $u^i(x)$ is an entire function, (2.1) is a special case of the following problem after renaming the function

$$\begin{cases} \Delta u + k^2 u = 0, & \mathbb{R}^2 \setminus \Gamma \\ \frac{\partial u}{\partial n} + \beta_1(x)u = f_1(x), & \Gamma^+ \\ \frac{\partial u}{\partial n} - \beta_2(x)u = f_2(x), & \Gamma^- \\ \frac{\partial u}{\partial |x|} - ik u(x) = o\left(\frac{1}{\sqrt{|x|}}\right), & |x| \rightarrow \infty \end{cases} \quad (2.2)$$

with $k = \Re k > 0$ and $\Im\beta_j(x) \leq 0$ for $j = 1, 2$, where the boundary conditions at the ends of arc Γ are not required.

Firstly, we introduce a function space so that we can describe the singularity of solution to (2.2). In this paper, Γ means the closed arc, that is, it contains the tips $x(a)$ and $x(b)$.

Definition 2.1. The function $u(x)$ belongs to the class \mathbb{K} , if it satisfies the following conditions:

- (1). $u \in C^2(\mathbb{R}^2 \setminus \Gamma)$, $u(x)$ is continuously extendable on the cut Γ from the left and right, $u(x)$ is continuous at $X := \{x(a), x(b)\}$, the ends of Γ ;
- (2). $\nabla u(x)$ is continuously extendable on the cut $\Gamma \setminus X$ from the left and right;
- (3). In the neighborhood of $x(d) \in X$ with $d = a, b$, there exists a constant $C > 0$ and $\varepsilon \in (-1, 0]$ such that

$$|\nabla u(x)| \leq C|x - x(d)|^\varepsilon, \quad x \rightarrow x(d).$$

The following well-posedness result for problem (2.2) has been proved in [9].

Theorem 2.2. *There exists a unique solution $u(x) \in \mathbb{K}$ of (2.2), provided $\Gamma \in C^{2,\lambda}$ and $\beta_1, \beta_2, f_1, f_2 \in C^{0,\lambda}[a, b]$ for $\lambda \in (0, 1]$.*

The proof for the uniqueness of solution is carried out using the standard energy method, noticing the radiation condition and the continuity of solution, especially on the tips of Γ . However, the existence of solution in \mathbb{K} is constructive. The main technique is to represent the solution by potential functions and then to prove the unique solvability of density functions such that the solution is in \mathbb{K} . Since such a construction scheme is crucial to our computational scheme, we state the main process and make the correspondent modification for the case that the arc Γ is represented by general parameter $s \in [a, b]$, rather than length arc. Such an modification is necessary to the singularity analysis of density functions.

Denote by $H_0^{(1)}(z)$ the Hankel function of the first kind of zero order. Consider the angular potential introduced in [11]

$$v[\mu_1](x) = \frac{i}{4} \int_{\Gamma} \mu_1(\sigma) V(x, \sigma) dl_{\sigma}, \quad x \in \mathbb{R}^2 \setminus \Gamma, \quad (2.3)$$

where arc length $dl_{\sigma} > 0$ as σ increases, and $V(\cdot, \sigma)$ is defined in $\mathbb{R}^2 \setminus \Gamma$ by an integral

$$V(x, \sigma) := \int_a^{\sigma} \frac{\partial H_0^{(1)}(k|x - y(\xi)|)}{\partial n(y(\xi))} |\dot{y}(\xi)| d\xi, \quad \sigma \in [a, b]$$

for $y(\xi) = (y_1(\xi), y_2(\xi)) \in \Gamma$, $|x - y(\xi)|$ is the Euclidian distance of $x, y(\xi)$.

Definition 2.3. We say that $\mu_1(\sigma) \in C_q^{\omega}[a, b]$ for $\omega \in (0, 1], q \in [0, 1)$, if $\mu_1(s)(s - a)^q(b - s)^q \in C^{0,\omega}[a, b]$. The norm is given by

$$\|\mu_1(s)\|_{C_q^{\omega}[a,b]} := \|\mu_1(s)(s - a)^q(b - s)^q\|_{C^{0,\omega}[a,b]}.$$

Inserting the expression of $V(x, \sigma)$ into (2.3) and integrating by parts yield ([11])

$$\begin{aligned} v[\mu_1](x) &= \frac{i}{4} \int_a^b \mu_1(\xi) |\dot{y}(\xi)| d\xi \int_a^b \frac{\partial H_0^{(1)}(k|x - y(\xi)|)}{\partial n(y)} |\dot{y}(\xi)| d\xi - \\ &\frac{i}{4} \int_a^b \int_a^{\sigma} \mu_1(\xi) |\dot{y}(\xi)| d\xi \frac{\partial H_0^{(1)}(k|x - y(\sigma)|)}{\partial n(y)} |\dot{y}(\sigma)| d\sigma. \end{aligned}$$

Since we will use $v[\mu_1](x)$ to construct $u \in \mathbb{K}$, so we need $v[\mu_1](\cdot) \in \mathbb{K}$, which means $v[\mu_1](x)$ should be continuous at two ends $x(a), x(b)$. However, it is shown in [13, Theorem 2(1)] that $\int_a^b \frac{\partial H_0^{(1)}(k|x-y(\xi)|)}{\partial n(y)} |\dot{y}(\xi)| d\xi$, the first term of the right-hand side, is not continuous at $x = x(a), x(b)$. To remove this difficulty, the following condition has been proposed in [11, 12]

$$\int_{\Gamma} \mu_1(\xi) dl_{\xi} = 0. \quad (2.4)$$

Under this condition, $v[\mu_1](x)$ given by (2.3) becomes

$$v[\mu_1](x) = -\frac{i}{4} \int_{\Gamma} \rho[\mu_1](\sigma) \frac{\partial H_0^{(1)}(k|x-y(\sigma)|)}{\partial n(y)} dl_{\sigma}, \quad (2.5)$$

which is in \mathbb{K} (see [13, Theorem 2]) and solves the Helmholtz equation with radiation condition, where we introduce

$$\rho[\mu_1](\sigma) = \int_a^{\sigma} \mu_1(\xi) |\dot{y}(\xi)| d\xi. \quad (2.6)$$

Obviously, under the condition (2.4), the angular potential (2.3) with density $\mu_1 \in C_q^{\omega}[a, b]$ becomes the double-layer potential (2.5) with density $\rho[\mu_1] \in C[a, b]$.

In [9], the solution to (2.2) in \mathbb{K} is constructed in the form of sum of an angular potential and single layer potential:

$$u[\mu_1, \mu_2](x) = v[\mu_1](x) + w[\mu_2](x), \quad (2.7)$$

where w is the single layer potential

$$w[\mu_2](x) = \frac{i}{4} \int_{\Gamma} \mu_2(\sigma) H_0^{(1)}(k|x-y(\sigma)|) dl_{\sigma}$$

with $\mu_2 \in C^{0, \lambda/4}[a, b]$, and $\mu_1 \in C_{1/2}^{\lambda/4}[a, b]$ satisfying (2.4). For these density functions, (2.7) gives a function in \mathbb{K} solving (2.2), except the boundary condition on Γ^{\pm} . These conditions are used in [9] to determine μ_1, μ_2 . To this end, let us introduce some known kernel functions from [9]. Denote by $\phi_0(x, y)$ the angle between $\vec{x}\vec{y}$ and $n(x)$ and define

$$\begin{cases} h(z) = H_0^{(1)}(z) - \frac{2i}{\pi} \ln \frac{z}{k}, \quad V_0(x, \sigma) = \int_a^{\sigma} \frac{\partial h(k|x-y(\xi)|)}{\partial n(y)} |\dot{y}(\xi)| d\xi \\ A_{22}^{\pm}(s, \sigma) = \frac{i}{4} (\beta_2(s) \pm \beta_1(s)) H_0^{(1)}(k|x(s) - y(\sigma)|) \\ Y_{11}(s, \sigma) = \frac{1}{\pi} \left(\frac{\sin \phi_0(x(s), y(\sigma))}{|x(s) - y(\sigma)|} - \frac{1}{(\sigma - s)|\dot{y}(\sigma)|} \right) - \frac{i}{2} \frac{\partial V_0(x(s), \sigma)}{\partial n(x)} - \frac{i}{4} (\beta_1(s) - \beta_2(s)) V(x(s), \sigma) \\ Y_{12}(s, \sigma) = -\frac{i}{2} \frac{\partial H_0^{(1)}(k|x(s) - y(\sigma)|)}{\partial n(x)}, \quad Y[\mu_2](s) = \int_{\Gamma} \mu_2(\sigma) A_{22}^{-}(s, \sigma) dl_{\sigma} \\ A_{21}(s, \sigma) = \frac{i}{4} (\beta_1(s) + \beta_2(s)) V(x(s), \sigma). \end{cases} \quad (2.8)$$

Now we have the following

Theorem 2.4. *Let $\Gamma \in C^{2, \lambda}$, $\beta_1, \beta_2, f_1, f_2 \in C^{0, \lambda}[a, b]$ with $\lambda \in (0, 1]$. If $\mu_1(s) \in C_q^{\omega}[a, b]$ for $\omega \in (0, 1], q \in [0, 1)$ and $\mu_2(s) \in C^{0, \lambda/4}[a, b]$ satisfy (2.4) and the following system*

$$\begin{cases} \frac{1}{\pi} \int_a^b \mu_1(\sigma) \frac{1}{\sigma - s} d\sigma + \int_{\Gamma} \mu_1(\sigma) Y_{11}(s, \sigma) dl_{\sigma} + \int_{\Gamma} \mu_2(\sigma) Y_{12}(s, \sigma) dl_{\sigma} + Y[\mu_2](s) - \\ \quad \frac{1}{2} (\beta_1(s) + \beta_2(s)) \rho[\mu_1](s) = -(f_1(s) + f_2(s)) \\ \mu_2(s) + \int_{\Gamma} \mu_1(\sigma) A_{21}(s, \sigma) dl_{\sigma} + \int_{\Gamma} \mu_2(\sigma) A_{22}^{+}(s, \sigma) dl_{\sigma} + \\ \quad \frac{1}{2} (\beta_1(s) - \beta_2(s)) \rho[\mu_1](s) = f_1(s) - f_2(s), \end{cases} \quad (2.9)$$

then $u(x)$ given by (2.7) belongs to \mathbb{K} and solves the scattering problem (2.2).

Please notice the different expression of the first term in Y_{11} from that arising in [9, 10], which is due to the situation considered here that s may not be the arc length.

Proof. It is easy to see that the boundary condition in (2.2) is equivalent to

$$\begin{cases} \frac{\partial u}{\partial n}|_{x(s) \in \Gamma^+} + \frac{\partial u}{\partial n}|_{x(s) \in \Gamma^-} + (\beta_1 u)|_{x(s) \in \Gamma^+} - (\beta_2 u)|_{x(s) \in \Gamma^-} = f_1(s) + f_2(s), \\ \frac{\partial u}{\partial n}|_{x(s) \in \Gamma^+} - \frac{\partial u}{\partial n}|_{x(s) \in \Gamma^-} + (\beta_1 u)|_{x(s) \in \Gamma^+} + (\beta_2 u)|_{x(s) \in \Gamma^-} = f_1(s) - f_2(s). \end{cases} \quad (2.10)$$

Since $w[\mu_2](x)$ is a single-layer potential with density function μ_2 , it is continuous in Γ and the jump relation of its normal derivative is standard [11, Theorem 5]. Now let us consider the angular potential $v[\mu_1](x)$, which is essentially a double-layer potential under the condition (2.4). The properties of the angular potential have been studied in [11] in details. It follows from [11, Theorem 5] that as $x \rightarrow x(s) \in \Gamma^\pm$ the normal derivative of the angular potential has the following limiting values on Γ^+ and on Γ^-

$$\lim_{x \rightarrow x(s) \in \Gamma^\pm} \frac{\partial v[\mu_1]}{\partial n(x)}(x) = -\frac{1}{2\pi} \int_{\Gamma} \mu_1(\sigma) \frac{\sin(\phi_0(x(s), y(\sigma)))}{|x(s) - y(\sigma)|} dl_\sigma + \frac{i}{4} \int_{\Gamma} \mu_1(\sigma) \frac{\partial V_0(x(s), \sigma)}{\partial n(x(s))} dl_\sigma, \quad (2.11)$$

where

$$\sin \phi_0(x(s), y(\sigma)) = -\frac{(x(s) - y(\sigma)) \cdot \dot{x}(s)}{|x(s) - y(\sigma)| |\dot{x}(s)|},$$

and $\phi_0(x(s), y(\sigma))$ is the angle between \overrightarrow{xy} and $n(x)$.

Substituting $u(x)$ from (2.7) into the boundary conditions (2.10) and using this key relation for the angular potential, we observe that the density functions (μ_1, μ_2) should obey the following integral equations, which have been derived in [9]

$$\begin{cases} -\frac{1}{\pi} \int_{\Gamma} \mu_1(\sigma) \frac{\sin \phi_0(x(s), y(\sigma))}{|x(s) - y(\sigma)|} dl_\sigma + \frac{i}{2} \int_{\Gamma} \mu_1(\sigma) \frac{\partial V_0(x(s), \sigma)}{\partial n(x)} dl_\sigma + \\ \frac{i}{2} \int_{\Gamma} \mu_2(\sigma) \frac{\partial H_0^{(1)}(k|x(s) - y(\sigma)|)}{\partial n(x)} dl_\sigma + \frac{1}{2} (\beta_1(s) + \beta_2(s)) \rho[\mu_1](s) + \\ \frac{i}{4} (\beta_1(s) - \beta_2(s)) \left[\int_{\Gamma} \mu_2(\sigma) H_0^{(1)}(k|x(s) - y(\sigma)|) dl_\sigma + \int_{\Gamma} \mu_1(\sigma) V(x(s), \sigma) dl_\sigma \right] = \\ f_1(s) + f_2(s), \\ \mu_2(s) + \frac{1}{2} (\beta_1(s) - \beta_2(s)) \rho[\mu_1](s) + \\ \frac{i}{4} (\beta_1(s) + \beta_2(s)) \left[\int_{\Gamma} \mu_2(\sigma) H_0^{(1)}(k|x(s) - y(\sigma)|) dl_\sigma + \int_{\Gamma} \mu_1(\sigma) V(x(s), \sigma) dl_\sigma \right] = \\ f_1(s) - f_2(s). \end{cases}$$

Finally by decomposing the kernel in the first integral as

$$\frac{\sin \phi_0(x(s), y(\sigma))}{|x(s) - y(\sigma)|} = \frac{1}{(\sigma - s) |\dot{y}(\sigma)|} + \frac{\sin \phi_0(x(s), y(\sigma))}{|x(s) - y(\sigma)|} - \frac{1}{(\sigma - s) |\dot{y}(\sigma)|}$$

and inserting it into the first equation, we derive the first equation in (2.9) noticing $dl_\sigma = |\dot{y}(\sigma)| d\sigma$. The second equation in (2.9) is obtained directly. \square

Let $\Gamma \in C^{2,\lambda}$, $\lambda \in (0, 1]$. The regularity for the kernels in (2.9), except for $\frac{\sin \phi_0(x(s), y(\sigma))}{|x(s) - y(\sigma)|} - \frac{1}{(\sigma - s)|\dot{y}(\sigma)|}$, is thoroughly analyzed in [9] with the help of the smoothness properties of $h(z)$. Now we study regularity of this kernel. Using the same arguments as that in Lemmas 2 and 3 in [11], it can be shown that

$$\left(\frac{\sin \phi_0(x(s), y(\sigma))}{|x(s) - y(\sigma)|} - \frac{1}{(\sigma - s)|\dot{x}(s)|} \right) \in C^{0,\lambda}([a, b] \times [a, b]).$$

Therefore, it follows from the decomposition

$$\frac{\sin \phi_0(x(s), y(\sigma))}{|x(s) - y(\sigma)|} - \frac{1}{(\sigma - s)|\dot{y}(\sigma)|} = \frac{\sin \phi_0(x(s), y(\sigma))}{|x(s) - y(\sigma)|} - \frac{1}{(\sigma - s)|\dot{x}(s)|} + \frac{|\dot{y}(\sigma)| - |\dot{x}(s)|}{(\sigma - s)|\dot{x}(s)||\dot{y}(\sigma)|}$$

that $\frac{\sin \phi_0(x(s), y(\sigma))}{|x(s) - y(\sigma)|} - \frac{1}{(\sigma - s)|\dot{y}(\sigma)|}$ is also in $C^{0,\lambda}([a, b]^2)$, noticing $\frac{|\dot{y}(\sigma)| - |\dot{x}(s)|}{(\sigma - s)|\dot{x}(s)||\dot{y}(\sigma)|} \in C^{0,\lambda}([a, b]^2)$. In addition, if $\Gamma \in C^4$, then from the same arguments it follows that

$$\left(\frac{\sin \phi_0(x(s), y(\sigma))}{|x(s) - y(\sigma)|} - \frac{1}{(\sigma - s)|\dot{y}(\sigma)|} \right) \in C^2([a, b]^2).$$

The regularity of kernels in the system (2.9) will be used in deriving the discrete form of this system.

It is proved in [9] that under conditions of Theorem 2.4, the system (2.9), (2.4) has unique solution $(\mu_1(s), \mu_2(s))$, where $\mu_1(s) \in C^{\lambda/4}[a, b]$, $\mu_2(s) \in C^{0,\lambda/4}[a, b]$. Define

$$\mathcal{Q}_{1/2}(s) = (s - a)^{1/2}(b - s)^{1/2} \quad (2.12)$$

and take the transform

$$\mu_1(s) = \frac{\mu_{1*}(s)}{\mathcal{Q}_{1/2}(s)}, \quad (2.13)$$

then (2.9) can be rewritten for new unknown (μ_{1*}, μ_2) as

$$\begin{cases} \frac{1}{\pi} \int_a^b \frac{\mu_{1*}(\sigma)}{\mathcal{Q}_{1/2}(\sigma)(\sigma - s)} d\sigma + \int_{\Gamma} \frac{\mu_{1*}(\sigma)}{\mathcal{Q}_{1/2}(\sigma)} Y_{11}(s, \sigma) dl_{\sigma} + \int_{\Gamma} \mu_2(\sigma) Y_{12}(s, \sigma) dl_{\sigma} + Y[\mu_2](s) - \\ \quad \frac{1}{2}(\beta_1(s) + \beta_2(s))\rho[\frac{\mu_{1*}}{\mathcal{Q}_{1/2}}](s) = -(f_1(s) + f_2(s)) \\ \mu_2(s) + \int_{\Gamma} \frac{\mu_{1*}(\sigma)}{\mathcal{Q}_{1/2}(\sigma)} A_{21}(s, \sigma) dl_{\sigma} + \int_{\Gamma} \mu_2(\sigma) A_{22}^+(s, \sigma) dl_{\sigma} + \\ \quad \frac{1}{2}(\beta_1(s) - \beta_2(s))\rho[\frac{\mu_{1*}}{\mathcal{Q}_{1/2}}](s) = f_1(s) - f_2(s). \end{cases} \quad (2.14)$$

Under the transform (2.13), (2.4) becomes

$$\int_a^b \frac{\mu_{1*}(s)|\dot{y}(s)|}{\mathcal{Q}_{1/2}(s)} ds = 0. \quad (2.15)$$

Equations (2.14) and (2.15) constitute a system for determining (μ_{1*}, μ_2) . It follows from [9] that this system is uniquely solvable in the function space $C^{0,\lambda/4}[a, b] \times C^{0,\lambda/4}[a, b]$ under the regularity $f_1, f_2, \beta_1, \beta_2 \in C^{0,\lambda}[a, b], \Gamma \in C^{2,\lambda}$.

Let $\Gamma \in C^4$. For the computation of

$$\frac{\partial V_0(x(s), \sigma)}{\partial n(x)} = \int_a^{\sigma} \frac{\partial}{\partial n(x)} \frac{\partial h(k|x(s) - y(\xi)|)}{\partial n(y)} |\dot{y}(\xi)| d\xi,$$

we need the singularity decomposition

$$\frac{\partial}{\partial n(x)} \frac{\partial h(k|x(s) - y(\xi))}{\partial n(y)} = \frac{i}{\pi} k^2 \ln |s - \xi| + g(s, \xi), \quad (2.16)$$

where the function $g(s, \xi)$ has the expression

$$\begin{cases} g(s, \xi) = -k^2 h''(k|x(s) - y(\xi)) \frac{(x(s)-y(\xi)) \cdot \dot{x}(s)^\perp}{|x(s)-y(\xi)| |\dot{x}(s)|} \frac{(x(s)-y(\xi)) \cdot \dot{y}(\xi)^\perp}{|x(s)-y(\xi)| |\dot{y}(\xi)|} - \\ \quad kh'(k|x(s) - y(\xi)) \frac{(x(s)-y(\xi)) \cdot \dot{x}(s)}{|x(s)-y(\xi)| |\dot{x}(s)|} \frac{(x(s)-y(\xi)) \cdot \dot{y}(\xi)}{|x(s)-y(\xi)| |\dot{y}(\xi)|} \frac{1}{|x(s)-y(\xi)|} - \frac{i}{\pi} k^2 \ln |s - \xi|. \\ h''(z) = -\frac{1}{z} H_1^{(1)}(z) + H_2^{(1)}(z) + \frac{2i}{\pi} \frac{1}{z^2} = -\frac{i}{\pi} \ln z + C + O(z^2 \ln z) \\ h'(z) = -H_1^{(1)}(z) - \frac{2i}{\pi} \frac{1}{z} = -\frac{i}{\pi} z \ln z + \text{constant } z + O(z^3 \ln z). \end{cases}$$

from the direct computations. Here $\dot{x}(s)^\perp = (\dot{x}_2(s), -\dot{x}_1(s))$, $\dot{y}(\xi)^\perp = (\dot{y}_2(\xi), -\dot{y}_1(\xi))$. It follows from proof of Lemma 2 in [12] that $g(s, \xi) = \tilde{g}(s, \xi) + \text{Constant } (s - \xi)^2 \ln |s - \xi|$ with $\tilde{g}(s, \xi) \in C^2([a, b]^2)$. Such a decomposition will be used in the discretization process. The remaining integrals are easy to handle.

Using these relations, all integrals in the final equations (2.14) and (2.15) will be changed into the integrals with respect to non arc length parameter s . Once (μ_{1*}, μ_2) is solved from the above system, the solution u can be computed from the potentials. However, many integrals in the above system with weak singularity should be discretized carefully so that the high accuracy can be obtained. These issue will be discussed in the next section.

3 Production of discrete system

Now we compute each integral in the system (2.14) and (2.15), such that a finite linear system can be produced. To guarantee the numerical accuracy, we assume that $\Gamma \in C^4$; $\beta_1, \beta_2, f_1, f_2 \in C^2[a, b]$. We will look for the numerical solution $(\mu_{1*}(s), \mu_2(s))$ of the system (2.14) and (2.15) in assumption that $\mu_{1*}(s), \mu_2(s) \in C^2[a, b]$.

In our computation, we set $z_j = a + (b - a)/M \times j := a + \tau \times j$ with $j = 0, 1, \dots, M$ to divide $[a, b]$ into M -subintervals, and take $s_j := (z_{j-1} + z_j)/2$ for $j = 1, \dots, M$, i.e. the middle point of the interval $[z_{j-1}, z_j]$.

To compute the integrals, we need the following standard Lemma.

Lemma 3.1. *Suppose $F(\sigma) \in C^2[a, b]$. Then we have the estimates*

$$\begin{cases} \int_{z_0}^{z_1} \frac{F(\sigma)}{\sqrt{\sigma-a}\sqrt{b-\sigma}} d\sigma = \left(\frac{4}{3} \frac{F(z_0)}{\sqrt{b-z_0}} + \frac{2}{3} \frac{F(z_1)}{\sqrt{b-z_1}} \right) \sqrt{\tau} + O(\tau^{5/2}), \\ \int_{z_{M-1}}^{z_M} \frac{F(\sigma)}{\sqrt{\sigma-a}\sqrt{b-\sigma}} d\sigma = \left(\frac{2}{3} \frac{F(z_{M-1})}{\sqrt{z_{M-1}-a}} + \frac{4}{3} \frac{F(z_M)}{\sqrt{z_M-a}} \right) \sqrt{\tau} + O(\tau^{5/2}) \\ \int_{z_1}^{z_{M-1}} \frac{F(\sigma)}{\sqrt{\sigma-a}\sqrt{b-\sigma}} d\sigma = \sum_{j=2}^{M-1} \frac{\tau}{2} \left(\frac{F(z_{j-1})}{\sqrt{z_{j-1}-a}\sqrt{b-z_{j-1}}} + \frac{F(z_j)}{\sqrt{z_j-a}\sqrt{b-z_j}} \right) + O(\tau^2). \end{cases}$$

Step 1. Compute the first integral $\mathcal{T}_1(s) := \int_a^b \frac{\mu_{1*}(\sigma)}{\mathcal{Q}_{1/2}(\sigma)(\sigma-s)} d\sigma$, which is a Cauchy singular integral.

Use the decomposition

$$\mathcal{T}_1(s) := \int_a^b \frac{\mu_{1*}(\sigma)}{\mathcal{Q}_{1/2}(\sigma)(\sigma-s)} d\sigma = \int_{z_0}^{z_1} + \int_{z_1}^{z_{M-1}} + \int_{z_{M-1}}^{z_M} \quad (3.1)$$

and compute the integrals at $s = s_n$ ($n = 1, \dots, M$) in terms of Lemma 3.1 approximately.

For $n = 1, \dots, M$, the second term in the right-hand side of (3.1) can be computed by the method of discrete vortices developed in [1, 17, 18], i.e.

$$\int_{z_1}^{z_{M-1}} = \sum_{m=2}^{M-1} \frac{1}{2} \tau \left[\frac{\mu_{1*}(z_{m-1})}{\mathcal{Q}_{1/2}(z_{m-1})(z_{m-1} - s_n)} + \frac{\mu_{1*}(z_m)}{\mathcal{Q}_{1/2}(z_m)(z_m - s_n)} \right] + O(\tau^2). \quad (3.2)$$

For the first and the third term in the right-hand side of (3.1), it follows from Lemma 3.1 that

$$\begin{cases} \int_{z_0}^{z_1} = \frac{2}{3} \left[\frac{2\mu_{1*}(z_0)}{\sqrt{M}(z_0 - s_n)} + \frac{\mu_{1*}(z_1)}{\sqrt{M-1}(z_1 - s_n)} \right] + O(\tau^{5/2}), & n = 2, 3, \dots, M. \\ \int_{z_{M-1}}^{z_M} = \frac{2}{3} \left[\frac{2\mu_{1*}(z_M)}{\sqrt{M}(z_M - s_n)} + \frac{\mu_{1*}(z_{M-1})}{\sqrt{M-1}(z_{M-1} - s_n)} \right] + O(\tau^{5/2}), & n = 1, 3, \dots, M-1. \end{cases} \quad (3.3)$$

Now let us compute the following two integrals:

$$I_1(s_1) := \int_{z_0}^{z_1} \frac{\mu_{1*}(\sigma)}{\mathcal{Q}_{1/2}(\sigma)(\sigma - s_1)} d\sigma, \quad I_M(s_M) := \int_{z_{M-1}}^{z_M} \frac{\mu_{1*}(\sigma)}{\mathcal{Q}_{1/2}(\sigma)(\sigma - s_M)} d\sigma.$$

For computing $I_1(s_1)$, we use the linear approximation for $\sigma \in [z_0, z_1]$ to get

$$\frac{1}{\sqrt{b-\sigma}} \mu_{1*}(\sigma) = \frac{\mu_{1*}(z_0)}{\sqrt{b-z_0}} + \frac{\sigma - z_0}{\tau} \left(\frac{\mu_{1*}(z_1)}{\sqrt{b-z_1}} - \frac{\mu_{1*}(z_0)}{\sqrt{b-z_0}} \right) + O(\tau^2).$$

Since

$$\int_{z_0}^{z_1} \frac{1}{\sqrt{\sigma - z_0}(\sigma - s_1)} d\sigma = P, \quad \int_{z_0}^{z_1} \frac{\sigma - z_0}{\sqrt{\sigma - z_0}(\sigma - s_1)} d\sigma = 2\sqrt{\tau} + (s_1 - z_0)P$$

with $P := \sqrt{2/\tau} \ln \left| \frac{\sqrt{2}-1}{\sqrt{2}+1} \right|$, we finally obtain

$$I_1(s_1) = r_{11}\mu_{1*}(z_0) + r_{21}\mu_{1*}(z_1) + O(\tau^{3/2}) \quad (3.4)$$

with the weights $r_{11} = \frac{1}{\sqrt{b-z_0}}(P - \frac{2}{\sqrt{\tau}} - \frac{s_1-a}{\tau}P)$, $r_{21} = \frac{1}{\sqrt{b-z_1}}(\frac{2}{\sqrt{\tau}} + \frac{s_1-a}{\tau}P)$. By a similar treatment, we obtain

$$I_M(s_M) = r_{1M}\mu_{1*}(z_{M-1}) + r_{2M}\mu_{1*}(z_M) + O(\tau^{3/2}) \quad (3.5)$$

with the weights $r_{1M} = \frac{1}{\sqrt{z_{M-1}-a}}(-\frac{2}{\sqrt{\tau}} - \frac{b-s_M}{\tau}P)$, $r_{2M} = \frac{1}{\sqrt{z_M-a}}(-P + \frac{2}{\sqrt{\tau}} + \frac{b-s_M}{\tau}P)$.

Conclusion. The values of $\mathcal{T}_1(s_n)$ are given by

$$\mathcal{T}_1(s_n) = \begin{cases} r_{11}\mu_{1*}(z_0) + r_{21}\mu_{1*}(z_1) + \\ \frac{2}{3} \left[\frac{2\mu_{1*}(z_M)}{\sqrt{M}(z_M - s_1)} + \frac{\mu_{1*}(z_{M-1})}{\sqrt{M-1}(z_{M-1} - s_1)} \right] + \\ \sum_{m=2}^{M-1} \frac{1}{2} \tau \left[\frac{\mu_{1*}(z_{m-1})}{\mathcal{Q}_{1/2}(z_{m-1})(z_{m-1} - s_1)} + \frac{\mu_{1*}(z_m)}{\mathcal{Q}_{1/2}(z_m)(z_m - s_1)} \right], & n = 1 \\ \frac{2}{3} \left[\frac{2\mu_{1*}(z_0)}{\sqrt{M}(z_0 - s_n)} + \frac{\mu_{1*}(z_1)}{\sqrt{M-1}(z_1 - s_n)} \right] + \\ \frac{2}{3} \left[\frac{2\mu_{1*}(z_M)}{\sqrt{M}(z_M - s_n)} + \frac{\mu_{1*}(z_{M-1})}{\sqrt{M-1}(z_{M-1} - s_n)} \right] + \\ \sum_{m=2}^{M-1} \frac{1}{2} \tau \left[\frac{\mu_{1*}(z_{m-1})}{\mathcal{Q}_{1/2}(z_{m-1})(z_{m-1} - s_n)} + \frac{\mu_{1*}(z_m)}{\mathcal{Q}_{1/2}(z_m)(z_m - s_n)} \right], & n = 2, \dots, M-1 \\ \frac{2}{3} \left[\frac{2\mu_{1*}(z_0)}{\sqrt{M}(z_0 - s_M)} + \frac{\mu_{1*}(z_1)}{\sqrt{M-1}(z_1 - s_M)} \right] + \\ r_{1M}\mu_{1*}(z_{M-1}) + r_{2M}\mu_{1*}(z_M) + \\ \sum_{m=2}^{M-1} \frac{1}{2} \tau \left[\frac{\mu_{1*}(z_{m-1})}{\mathcal{Q}_{1/2}(z_{m-1})(z_{m-1} - s_M)} + \frac{\mu_{1*}(z_m)}{\mathcal{Q}_{1/2}(z_m)(z_m - s_M)} \right], & n = M \end{cases} \quad (3.6)$$

The accuracy of this integral is $O(\tau^{3/2})$.

Step 2. Compute $\mathcal{T}_2(s) := \int_{\Gamma} \frac{\mu_{1*}(\sigma)}{\mathcal{Q}_{1/2}(\sigma)} Y_{11}(s, \sigma) dl_{\sigma}$.

We still use the decomposition

$$\mathcal{T}_2(s_n) = \sum_{m=1}^M \int_{z_{m-1}}^{z_m} \frac{\mu_{1*}(\sigma)}{\mathcal{Q}_{1/2}(\sigma)} Y_{11}(s_n, \sigma) |\dot{x}(\sigma)| d\sigma = \sum_{m=1, m \neq n}^M \int_{z_{m-1}}^{z_m} + \int_{z_{n-1}}^{z_n}.$$

Since $Y_{11}(s, \sigma)$ is not smooth for $s = \sigma$, we need to compute

$$\int_{z_{n-1}}^{z_n} \frac{\mu_{1*}(\sigma)}{\mathcal{Q}_{1/2}(\sigma)} Y_{11}(s_n, \sigma) |\dot{x}(\sigma)| d\sigma.$$

In fact, it follows from the properties of functions presented in [11, 12] that

$$Y_{11}(s_n, \sigma) = \tilde{Y}_{11}(s_n, \sigma) + \frac{1}{2\pi} k^2 (\sigma - s_n) \ln |\sigma - s_n|$$

with $\tilde{Y}_{11} \in C^2(\Gamma \times \Gamma)$. We Notice that

$$\int_{z_{n-1}}^{z_n} \frac{\mu_{1*}(\sigma) |\dot{x}(\sigma)|}{\mathcal{Q}_{1/2}(\sigma)} (\sigma - s_n) \ln |\sigma - s_n| d\sigma = O(\tau \ln \tau) \int_{z_{n-1}}^{z_n} \frac{1}{\mathcal{Q}_{1/2}(\sigma)} d\sigma = O(\tau^{3/2} \ln \tau)$$

for $n = 1, \dots, M$. This means that the integral of the weakly singular part can be considered as the truncation error. That is,

$$\int_{z_{n-1}}^{z_n} \frac{\mu_{1*}(\sigma)}{\mathcal{Q}_{1/2}(\sigma)} Y_{11}(s_n, \sigma) |\dot{x}(\sigma)| d\sigma \approx \int_{z_{n-1}}^{z_n} \frac{\mu_{1*}(\sigma)}{\mathcal{Q}_{1/2}(\sigma)} \tilde{Y}_{11}(s_n, \sigma) |\dot{x}(\sigma)| d\sigma,$$

where the integral is computed by the previous method. Finally, we obtain the approximation

$$\mathcal{T}_2(s_n) = \sum_{m=1}^M \int_{z_{m-1}}^{z_m} \frac{\mu_{1*}(\sigma)}{\mathcal{Q}_{1/2}(\sigma)} Y_{11}(s_n, \sigma) |\dot{x}(\sigma)| d\sigma + O(\tau^{3/2} \ln \tau),$$

where the integral can be computed as if Y_{11} is a smooth function. That is,

$$\int_{z_{m-1}}^{z_m} \frac{\mu_{1*}(\sigma)}{\mathcal{Q}_{1/2}(\sigma)} Y_{11}(s_n, \sigma) d\sigma = p_{1m} \mu_{1*}(z_{m-1}) Y_{11}(s_n, z_{m-1}) + p_{2m} \mu_{1*}(z_m) Y_{11}(s_n, z_m) + \varepsilon_{n,m}(\tau) \quad (3.7)$$

with the weights

$$p_{1m} = \frac{\tau |\dot{x}(z_{m-1})|}{2\mathcal{Q}_{1/2}(z_{m-1})}, \quad p_{2m} = \frac{\tau |\dot{x}(z_m)|}{2\mathcal{Q}_{1/2}(z_m)}, \quad m = 2, \dots, M-1. \quad (3.8)$$

The coefficients $(p_{11}, p_{21}), (p_{1M}, p_{2M})$ can be computed again from Lemma 3.1:

$$\begin{cases} p_{11} = \frac{4}{3} \frac{\sqrt{\tau} |\dot{x}(z_0)|}{\sqrt{b-z_0}}, & p_{21} = \frac{2}{3} \frac{\sqrt{\tau} |\dot{x}(z_1)|}{\sqrt{b-z_1}}. \\ p_{1M} = \frac{2}{3} \frac{\sqrt{\tau} |\dot{x}(z_{M-1})|}{\sqrt{z_{M-1}-a}}, & p_{2M} = \frac{4}{3} \frac{\sqrt{\tau} |\dot{x}(z_M)|}{\sqrt{z_M-a}}. \end{cases} \quad (3.9)$$

We notice that $Y_{11}(s_n, z_m)$ for all $m = 0, 1, \dots, M$ and $n = 1, 2, \dots, M$ are well-defined due to $s_n \neq z_m$. The truncation error $\varepsilon_{l,m}(\tau)$ in (3.7) is given by

$$\varepsilon_{n,m}(\tau) = \begin{cases} O(\tau^{3/2} \ln \tau), & n = m = 1, \text{ or } n = m = M \\ O(\tau^2 \ln \tau), & n = m \text{ and } n \neq 1, M \\ O(\tau^{5/2}), & m = 1, M \text{ and } n = 2, \dots, M-1 \\ O(\tau^3), & \text{other cases.} \end{cases}$$

From the expression of Y_{11} , we need to compute

$$V(x(s_n), z_m) = k \int_{z_0}^{z_m} H_1^{(1)}(k|x(s_n) - y(\xi)|) \frac{(x(s_n) - y(\xi)) \cdot \dot{y}(\xi)^\perp}{|x(s_n) - y(\xi)|} d\xi := k \int_{z_0}^{z_m} F1(s_n, \xi) d\xi$$

for $m = 0, \dots, M$ and fixed $n = 1, \dots, M$. We use the asymptotic

$$H_1^{(1)}(z) = -\frac{2i}{\pi} \frac{1}{z} + \frac{i}{\pi\Gamma(2)} z \ln \frac{z}{2} + \text{Constant } z - \frac{i}{4\pi\Gamma(3)} z^3 \ln \frac{z}{2} + \dots$$

to compute this integral for $s_n \in (z_0, z_{m-1})$.

It follows from the proof of Lemma 2 in [11] that $F1(s, \xi) \in C^2([a, b]^2)$ for $\Gamma \in C^4$. Moreover, for more smooth Γ , the smoothness of the above function will also be increased. Therefore we know that $F1(s_n, \xi)$ for all ξ is, in fact, a smooth function with removable singularity if $\xi = s_n$. More precisely, $F1(s, \xi) = \tilde{F}_1(s, \xi) + \text{Constant } (s - \xi)^2 \ln |s - \xi|$ with $\tilde{F}_1(s, \xi) \in C^2([a, b]^2)$. Therefore $V(x(s_n), z_m)$ can be computed by standard formula with the understanding that

$$\int_{z_{l-1}}^{z_l} F1(s_n, \xi) d\xi = \frac{\tau}{2} [F1(s_n, z_{l-1}) + F1(s_n, z_l)], \quad l, n = 1, 2, \dots, M.$$

and we get finally $V(x(s_n), z_m)$.

Step 3. Compute $\mathcal{T}_3(s) := \int_\Gamma \mu_2(\sigma) Y_{12}(s, \sigma) dl_\sigma$ for $s = s_n$.

The function $Y_{12}(s, \sigma)$ has the same smoothness as that of $F1(s, \sigma)$ in the previous step, since

$$Y_{12}(s, \sigma) = -\frac{i}{2} \frac{\partial H_0^{(1)}(k|x(s) - y(\sigma)|)}{\partial n(x)} = \frac{ik}{2} H_1^{(1)}(k|x(s_n) - y(\sigma)|) \frac{(x(s) - y(\sigma)) \cdot \dot{x}(s)^\perp}{|x(s) - y(\sigma)| |\dot{x}(s)|},$$

which means that $Y_{12}(s, \sigma) = \tilde{Y}_{12}(s, \sigma) + \text{Constant } (s - \sigma)^2 \ln |s - \sigma|$ with $\tilde{Y}_{12}(s, \sigma) \in C^2(\Gamma \times \Gamma)$, see again the proof of Lemma 2 in [11].

For the integral $\mathcal{T}_3(s)$, we use the decomposition $\mathcal{T}_3(s_n) = \sum_{m=1}^M \int_{z_{m-1}}^{z_m} \mu_2(\sigma) Y_{12}(s_n, \sigma) |\dot{x}(\sigma)| d\sigma$ and the Taylor expansion

$$\mu_2(\sigma) Y_{12}(s_n, \sigma) = \mu_2(\sigma) Y_{12}(s_n, \sigma)|_{\sigma=s_m} + \frac{d}{d\sigma} \mu_2(\sigma) Y_{12}(s_n, \sigma)|_{\sigma=s_m} (\sigma - s_m) + \eta_{n,m}(\tau)$$

for $\sigma \in [z_{m-1}, z_m]$, where $\eta_{n,m}(\tau) = O(\tau^2)$ for $n \neq m$ and $\eta_{n,m}(\tau) = O(\tau^2 \ln \tau)$ for $n = m$. So we are led to

$$\mathcal{T}_3(s_n) = \tau \sum_{m=1}^M \mu_2(s_m) Y_{12}(s_n, s_m) |\dot{x}(s_m)| + O(\tau^2), \quad n = 1, 2, \dots, M, \quad (3.10)$$

noticing that s_m is the middle point of $[z_{m-1}, z_m]$. Since $Y_{12}(s, \sigma)$ is smooth with a removable singularity at $s = \sigma$, we can compute

$$Y_{12}(s_n, s_n) \approx \frac{1}{2}[Y_{12}(s_n, s_n - \tau/4) + Y_{12}(s_n, s_n + \tau/4)], \quad n = 1, \dots, M,$$

without changing the accuracy of (3.10).

Step 4. Compute

$$Y[\mu_2](s) = [\beta_2(s) - \beta_1(s)] \int_a^b \mu_2(\sigma) \frac{i}{4} H_0^{(1)}(k|x(s) - y(\sigma)|) |\dot{x}(\sigma)| d\sigma := [\beta_2(s) - \beta_1(s)] \mathcal{T}_4(s)$$

for $s = s_n$, which is an integral with weak singularity.

Using the singularity expansion of $H_0^{(1)}(z)$ at $z = 0$, it follows that

$$\frac{i}{4} H_0^{(1)}(k|x(s) - y(\sigma)|) = -\frac{1}{2\pi} \ln|s - \sigma| + \psi(|x(s) - y(\sigma)|)$$

with $\psi(|x(s) - y(\sigma)|) := \tilde{\psi}(|x(s) - y(\sigma)|) + \text{Constant} (s - \sigma)^2 \ln|s - \sigma|$, where $\tilde{\psi} \in C^2(\Gamma \times \Gamma)$ and we omit the dependence of functions $\psi, \tilde{\psi}$ on k . For the smooth part, we also have that

$$\int_a^b \mu_2(\sigma) \psi(|x(s_n) - y(\sigma)|) |\dot{x}(\sigma)| d\sigma = \tau \sum_{m=1}^M \mu_2(s_m) \psi(|x(s_n) - y(s_m)|) |\dot{x}(s_m)| + O(\tau^2).$$

Again, since $\psi(|x(s) - y(\sigma)|)$ is continuous, $\psi(|x(s_n) - y(s_n)|)$ can be evaluated by

$$\psi(|x(s_n) - y(s_n)|) \approx \frac{1}{2}[\psi(|x(s_n) - y(s_n - \frac{\tau}{4})|) + \psi(|x(s_n) - y(s_n + \frac{\tau}{4})|)].$$

For the singular term, we consider that

$$\begin{aligned} \int_a^b \mu_2(\sigma) \ln|s_n - \sigma| |\dot{x}(\sigma)| d\sigma &= \sum_{m=1}^M \int_{z_{m-1}}^{z_m} \mu_2(\sigma) \ln|s_n - \sigma| |\dot{x}(\sigma)| d\sigma \\ &= \tau \sum_{m=1, m \neq n}^M \mu_2(s_m) |\dot{x}(s_m)| \ln|s_n - s_m| + O(\tau^2) + \int_{z_{n-1}}^{z_n} \mu_2(\sigma) |\dot{x}(\sigma)| \ln|s_n - \sigma| d\sigma. \end{aligned}$$

The last integral can be compute by Taylor expansion and the facts $\int_{z_{n-1}}^{z_n} \ln|\sigma - s_n| d\sigma = \tau(\ln \frac{\tau}{2} - 1)$ and $\int_{z_{n-1}}^{z_n} (\sigma - s_n) \ln|\sigma - s_n| d\sigma = 0$:

$$\int_{z_{n-1}}^{z_n} \mu_2(\sigma) \ln|s_n - \sigma| |\dot{x}(\sigma)| d\sigma = \tau(\ln \frac{\tau}{2} - 1) \mu_2(s_n) |\dot{x}(s_n)| + O(\tau^3 \ln \tau).$$

Conclusion.

$$\begin{aligned} \mathcal{T}_4(s_n) &= \tau \sum_{m=1}^M \mu_2(s_m) |\dot{x}(s_m)| \psi(|x(s_n) - y(s_m)|) - \frac{\tau}{2\pi} (\ln \frac{\tau}{2} - 1) \mu_2(s_n) |\dot{x}(s_n)| - \\ &\quad \frac{\tau}{2\pi} \sum_{m=1, m \neq n}^M \mu_2(s_m) |\dot{x}(s_m)| \ln|s_n - s_m| + O(\tau^2). \end{aligned} \quad (3.11)$$

Step 5: Compute $\mathcal{T}_5(s_n) = \rho[\frac{\mu_{1*}}{Q_{1/2}}](s_n) = \int_a^{s_n} \frac{\mu_{1*}(\sigma)}{\sqrt{\sigma - a} \sqrt{b - \sigma}} |\dot{x}(\sigma)| d\sigma$ for $n = 1, \dots, M$.

Since $s_n < b$, only the singularity at $\sigma = a$ needs to be considered. Use the same decomposition and Lemma 3.1 but approximate $\frac{d}{d\sigma}(\mu_{1*}(\sigma)|\dot{x}(\sigma)|)_{z_{n-1}}$ by

$$\frac{d}{d\sigma}(\mu_{1*}(\sigma)|\dot{x}(\sigma)|)_{z_{n-1}} = \frac{\mu_{1*}(z_n)|\dot{x}(z_n)| - \mu_{1*}(z_{n-1})|\dot{x}(z_{n-1})|}{\tau} + O(\tau)$$

when considering the integral in $[z_{n-1}, s_n]$, we obtain

$$\mathcal{T}_5(s_n) = \begin{cases} \left[\sqrt{\frac{\tau}{2}} \frac{5}{3} \frac{\mu_{1*}(a)|\dot{x}(a)|}{\sqrt{b-a}} + \frac{1}{3} \frac{\mu_{1*}(z_1)|\dot{x}(z_1)|}{\sqrt{b-z_1}} \right] + O(\tau^{5/2}), & n = 1 \\ \left(\frac{4}{3} \frac{\mu_{1*}(a)|\dot{x}(a)|}{\sqrt{b-a}} + \frac{2}{3} \frac{\mu_{1*}(z_1)|\dot{x}(z_1)|}{\sqrt{b-z_1}} \right) \sqrt{\tau} + \\ c_{12} \mu_{1*}(z_1)|\dot{x}(z_1)| + c_{22} \frac{\mu_{1*}(z_2)|\dot{x}(z_2)| - \mu_{1*}(z_1)|\dot{x}(z_1)|}{\tau} + O(\tau^{5/2}), & n = 2. \\ \left(\frac{4}{3} \frac{\mu_{1*}(a)|\dot{x}(a)|}{\sqrt{b-a}} + \frac{2}{3} \frac{\mu_{1*}(z_1)|\dot{x}(z_1)|}{\sqrt{b-z_1}} \right) \sqrt{\tau} + \sum_{m=2}^{n-1} \frac{\tau}{2} \left(\frac{\mu_{1*}(z_{m-1})|\dot{x}(z_{m-1})|}{\sqrt{z_{m-1}-a}\sqrt{b-z_{m-1}}} + \frac{\mu_{1*}(z_m)|\dot{x}(z_m)|}{\sqrt{z_m-a}\sqrt{b-z_m}} \right) + \\ c_{1n} \mu_{1*}(z_{n-1})|\dot{x}(z_{n-1})| + c_{2n} \frac{\mu_{1*}(z_n)|\dot{x}(z_n)| - \mu_{1*}(z_{n-1})|\dot{x}(z_{n-1})|}{\tau} + O(\tau^2), & n = 3, \dots, M \end{cases}$$

where

$$\begin{cases} c_{1n} = \int_{z_{n-1}}^{s_n} \frac{1}{\sqrt{\sigma-a}\sqrt{b-\sigma}} d\sigma = \arcsin \frac{2\sigma-(b+a)}{b-a} \Big|_{z_{n-1}}^{s_n}, \\ c_{2n} = \int_{z_{n-1}}^{s_n} \frac{\sigma-z_{n-1}}{\sqrt{\sigma-a}\sqrt{b-\sigma}} d\sigma = \left[-\frac{1}{2}(a+b-2z_{n-1}) \arctan \frac{a+b-2\sigma}{2\sqrt{\sigma-a}\sqrt{b-\sigma}} - \sqrt{\sigma-a}\sqrt{b-\sigma} \right] \Big|_{z_{n-1}}^{s_n} \end{cases}$$

Step 6: Compute $\mathcal{T}_6(s_n) := \int_{\Gamma} \frac{\mu_{1*}(\sigma)}{Q_{1/2}(\sigma)} A_{21}(s_n, \sigma) dl_{\sigma}$.

Since A_{21} is smooth (see the computation of $V(x(s), \sigma)$ in step 2), we only need to consider the singularity at $\sigma = a, b$.

Using Lemma 3.1, we have

$$\begin{aligned} \mathcal{T}_6(s_n) &= \left(\frac{4}{3} \frac{\mu_{1*}(z_0)|\dot{x}(z_0)| A_{21}(s_n, z_0)}{\sqrt{b-z_0}} + \frac{2}{3} \frac{\mu_{1*}(z_1)|\dot{x}(z_1)| A_{21}(s_n, z_1)}{\sqrt{b-z_1}} \right) \sqrt{\tau} + \\ &\sum_{m=2}^{M-1} \frac{\tau}{2} \left(\frac{\mu_{1*}(z_{m-1})|\dot{x}(z_{m-1})| A_{21}(s_n, z_{m-1})}{\sqrt{z_{m-1}-a}\sqrt{b-z_{m-1}}} + \frac{\mu_{1*}(z_m)|\dot{x}(z_m)| A_{21}(s_n, z_m)}{\sqrt{z_m-a}\sqrt{b-z_m}} \right) + \\ &\left(\frac{2}{3} \frac{\mu_{1*}(z_{M-1})|\dot{x}(z_{M-1})| A_{21}(s_n, z_{M-1})}{\sqrt{z_{M-1}-a}} + \frac{4}{3} \frac{\mu_{1*}(z_M)|\dot{x}(z_M)| A_{21}(s_n, z_M)}{\sqrt{z_M-a}} \right) \sqrt{\tau} + O(\tau^2) \end{aligned}$$

Step 7: Compute $\mathcal{T}_7(s_n) := \int_{\Gamma} \mu_2(\sigma) A_{22}^+(s, \sigma) dl_{\sigma}$.

This computation is completely the same as that in Step 4 for $Y[\mu_2](s)$. That is,

$$\mathcal{T}_7(s_n) = [\beta_2(s_n) + \beta_1(s_n)] \mathcal{T}_4(s_n)$$

Step 8. Compute $\mathcal{T}_8 := \int_a^b \frac{\mu_{1*}(\sigma)}{Q_{1/2}(\sigma)} |\dot{x}(\sigma)| d\sigma$ in equation (2.15).

Using Lemma 3.1 and taking $F(\sigma) = \mu_{1*}(\sigma)|\dot{x}(\sigma)|$, we are led to

$$\begin{aligned} \mathcal{T}_8 &= \left(\frac{4}{3} \frac{\mu_{1*}(z_0)|\dot{x}(z_0)|}{\sqrt{b-z_0}} + \frac{2}{3} \frac{\mu_{1*}(z_1)|\dot{x}(z_1)|}{\sqrt{b-z_1}} \right) \sqrt{\tau} + \\ &\left(\frac{2}{3} \frac{\mu_{1*}(z_{M-1})|\dot{x}(z_{M-1})|}{\sqrt{z_{M-1}-a}} + \frac{4}{3} \frac{\mu_{1*}(z_M)|\dot{x}(z_M)|}{\sqrt{z_M-a}} \right) \sqrt{\tau} + \\ &\sum_{j=2}^{M-1} \frac{\tau}{2} \left(\frac{\mu_{1*}(z_{j-1})|\dot{x}(z_{j-1})|}{\sqrt{z_{j-1}-a}\sqrt{b-z_{j-1}}} + \frac{\mu_{1*}(z_j)|\dot{x}(z_j)|}{\sqrt{z_j-a}\sqrt{b-z_j}} \right) + O(\tau^2). \end{aligned} \quad (3.12)$$

Step 9. Compute $\frac{\partial V_0(x(s_m), z_j)}{\partial n(x)}$.

Using the decomposition (2.16), we have that

$$\frac{\partial V_0(x(s_m), z_j)}{\partial n(x)} = \int_{z_0}^{z_j} \left[\frac{i}{\pi} k^2 \ln |s_m - \xi| + g(s_m, \xi) \right] |\dot{y}(\xi)| d\xi$$

Therefore we can compute $\frac{\partial V_0(x(s_m), z_0)}{\partial n(x)} = 0$ and

$$\begin{aligned} \frac{\partial V_0(x(s_m), z_j)}{\partial n(x)} &= \sum_{l=1}^j \int_{z_{l-1}}^{z_l} \left[\frac{i}{\pi} k^2 \ln |s_m - \xi| + g(s_m, \xi) \right] |\dot{y}(\xi)| d\xi \\ &= \sum_{l=1, l \neq m}^j \int_{z_{l-1}}^{z_l} \left[\frac{i}{\pi} k^2 \ln |s_m - \xi| + g(s_m, \xi) \right] |\dot{y}(\xi)| d\xi + \\ &\quad \int_{z_{m-1}}^{z_m} g(s_m, \xi) |\dot{y}(\xi)| d\xi + \frac{i}{\pi} k^2 \tau \left(\ln \frac{\tau}{2} - 1 \right) |\dot{y}(s_m)| \end{aligned}$$

for $j = 1, \dots, M$ and $m \leq j$. For $m > j$, it follows that

$$\frac{\partial V_0(x(s_m), z_j)}{\partial n(x)} = \sum_{l=1}^j \int_{z_{l-1}}^{z_l} \left[\frac{i}{\pi} k^2 \ln |s_m - \xi| + g(s_m, \xi) \right] |\dot{y}(\xi)| d\xi.$$

Using all the above expressions, we can solve the linear algebra equations. The convergence rate of the solution could be tested by doubling the mesh number M , which will be shown in the following section.

4 Determination of the scattered wave by the density function

Using the scattered wave representation given in the previous section, we know that the scattered wave outside Γ can be computed from

$$u(x) = v[\mu_1](x) + w[\mu_2](x), \quad x \in \mathbb{R}^2 \setminus \Gamma, \quad (4.1)$$

where the angular potential

$$v[\mu_1](x) := \frac{i}{4} \int_{\Gamma} \mu_1(\sigma) V(x, \sigma) dl_{\sigma}, \quad (4.2)$$

and the single layer potential

$$w[\mu_2](x) := \frac{i}{4} \int_{\Gamma} \mu_2(\sigma) H_0^{(1)}(k|x - y(\sigma)|) dl_{\sigma}. \quad (4.3)$$

Although (4.2) can also be expressed by a double layer potential with respect to $\rho[\mu_1](x)$ due to (2.4), such an expression has more strong singularity near Γ compared with the angular potential. So we use (4.2) near Γ directly.

Assuming that the point x is situated far from Γ and using the asymptotic behavior of the Hankel function at infinity, we obtain

$$w[\mu_2](x) = \frac{e^{ik|x|}}{\sqrt{|x|}} \left[\frac{e^{i\pi/4}}{\sqrt{8\pi k}} \int_{\Gamma} \mu_2(\sigma) e^{-ik\hat{x}\cdot y(\sigma)} dl_{\sigma} + O\left(\frac{1}{|x|}\right) \right]$$

and

$$\begin{aligned} v[\mu_1](x) &= \frac{ik}{4} \int_{\Gamma} \rho[\mu_1](\sigma) H_1^{(1)}(k|x-y(\sigma)|) \frac{(y(\sigma)-x)\cdot\dot{y}(\sigma)^{\perp}}{|x-y(\sigma)||\dot{y}(\sigma)|} dl_{\sigma} \\ &= \frac{e^{ik|x|}}{\sqrt{|x|}} \left[e^{-i(\frac{\pi}{4}+\frac{\pi}{2})} \frac{-ik}{4} \sqrt{\frac{2}{\pi k}} \int_{\Gamma} \rho[\mu_1](\sigma) \frac{\hat{x}\cdot\dot{y}(\sigma)^{\perp}}{|\dot{y}(\sigma)|} e^{-ik\hat{x}\cdot y(\sigma)} dl_{\sigma} + O\left(\frac{1}{|x|}\right) \right] \end{aligned}$$

as $|x| \rightarrow \infty$. Notice that when we derived the asymptotic formula for the angular potential we used (2.4). Therefore it follows from these asymptotic and the definition of far-field pattern that the far-field of $u(x)$ is

$$u^{\infty}(\hat{x}) = \frac{e^{i\pi/4}}{\sqrt{8\pi k}} \int_{\Gamma} \left(\mu_2(\sigma) + ik\rho[\mu_1](\sigma) \frac{\hat{x}\cdot\dot{y}(\sigma)^{\perp}}{|\dot{y}(\sigma)|} \right) e^{-ik\hat{x}\cdot y(\sigma)} dl_{\sigma}, \quad \hat{x} = \frac{x}{|x|}. \quad (4.4)$$

Hence the direct scattering problem for an arc can be solved by (4.1)-(4.4) with $x \in \mathbb{R}^2 \setminus \Gamma$.

We set W to be closed smooth curve which contains Γ in its interior part. Denote by $W = \{x : x = w(t) : t \in [0, 2\pi]\}$ the parametrization of W , where we want to determine the scattered wave $u(x)$. Assume that W is subdivided by $w(t_j)$ for $j = 0, 1, \dots, 2M-1$. Since the integrands are smooth due to $w(t_j) \notin \Gamma$, it follows from (4.1)-(4.3) that

$$\begin{aligned} u(w(t_j)) &= \frac{i}{4} \sum_{l=1}^M \int_{z_{l-1}}^{z_l} [\mu_1(\sigma)V(w(t_j), \sigma) + \mu_2(\sigma)H_0^{(1)}(k|w(t_j)-y(\sigma))||\dot{y}(\sigma)|] d\sigma \\ &= \frac{i}{4} \sum_{l=1}^M \int_{z_{l-1}}^{z_l} \frac{\mu_{1*}(\sigma)}{\mathcal{Q}_{1/2}(\sigma)} V(w(t_j), \sigma) |\dot{y}(\sigma)| d\sigma + \\ &\quad \frac{i}{4} \sum_{l=1}^M \int_{z_{l-1}}^{z_l} \mu_2(\sigma) H_0^{(1)}(k|w(t_j)-y(\sigma)) |\dot{y}(\sigma)| d\sigma \end{aligned} \quad (4.5)$$

For the second term, it can be computed by

$$\sum_{l=1}^M \int_{z_{l-1}}^{z_l} \mu_2(\sigma) H_0^{(1)}(k|w(t_j)-y(\sigma)) |\dot{y}(\sigma)| d\sigma \approx \tau \sum_{l=1}^M \mu_2(s_l) H_0^{(1)}(k|w(t_j)-x(s_l)) |\dot{x}(s_l)|, \quad (4.6)$$

since the integrands are smooth for $w(t_j) \in W$. For the first integral, the weak singularity

appears in $\sigma = z(0) = a, \sigma = z(M) = b$, which can be computed using Lemma 3.1, i.e.,

$$\begin{aligned} & \sum_{l=1}^M \int_{z_{l-1}}^{z_l} \frac{\mu_{1*}(\sigma)}{\mathcal{Q}_{1/2}(\sigma)} V(w(t_j), \sigma) |\dot{y}(\sigma)| d\sigma \approx \int_{z_0}^{z_1} + \int_{z_{M-1}}^{z_M} + \sum_{l=2}^{M-1} \int_{z_{l-1}}^{z_l} \\ & \approx \frac{4|\dot{x}(z_0)|}{3\sqrt{M}} \mu_{1*}(z_0) V(w(t_j), z_0) + \frac{2|\dot{x}(z_1)|}{3\sqrt{M-1}} \mu_{1*}(z_1) V(w(t_j), z_1) + \\ & \frac{2|\dot{x}(z_{M-1})|}{3\sqrt{M-1}} \mu_{1*}(z_{M-1}) V(w(t_j), z_{M-1}) + \frac{4|\dot{x}(z_M)|}{3\sqrt{M}} \mu_{1*}(z_M) V(w(t_j), z_M) + \\ & \sum_{l=2}^{M-1} \frac{\tau}{2} \left(\frac{|\dot{x}(z_{l-1})|}{\mathcal{Q}_{1/2}(z_{l-1})} \mu_{1*}(z_{l-1}) V(w(t_j), z_{l-1}) + \frac{|\dot{x}(z_l)|}{\mathcal{Q}_{1/2}(z_l)} \mu_{1*}(z_l) V(w(t_j), z_l) \right) \end{aligned} \quad (4.7)$$

with $V(w(t_j), z_0) = 0$. Therefore the scattered wave can be computed from (4.5) to (4.7).

As for the far-field pattern of the scattered wave, its discrete form for computation is

$$u_{Num}^\infty(\hat{x}) \approx \frac{e^{i\pi/4\tau}}{\sqrt{8\pi k}} \sum_{l=1}^M \left[\mu_2(s_l) |\dot{y}(s_l)| + ik \int_a^{s_l} \frac{\mu_{1*}(\xi) |\dot{x}(\xi)|}{\mathcal{Q}_{1/2}(\xi)} d\xi \hat{x} \cdot \dot{y}(s_l)^\perp \right] e^{-ik\hat{x} \cdot y(s_l)} \quad (4.8)$$

from (4.4). Again, the integral $\int_a^{s_l} \frac{\mu_{1*}(\xi) |\dot{x}(\xi)|}{\mathcal{Q}_{1/2}(\xi)} d\xi$ has weak singularity at $\xi = a$ for $l = 1, \dots, M$, which can be computed by previous way. That is,

$$\int_a^{s_l} \frac{f(\xi)}{\sqrt{\xi-a}} d\xi \approx \begin{cases} [\frac{5}{3}f(z_0) + \frac{1}{3}f(z_1)]\sqrt{\frac{\tau}{2}}, & l = 1 \\ \int_a^{s_1} + \sum_{j=1}^{l-1} \int_{z_j-\frac{\tau}{2}}^{z_j+\frac{\tau}{2}} = [\frac{5}{3}f(z_0) + \frac{1}{3}f(z_1)]\sqrt{\frac{\tau}{2}} + \sum_{j=1}^{l-1} \frac{f(z_j)}{\sqrt{z_j-a}}\tau, & l = 2, \dots, M \end{cases}$$

Now we construct a model problem to test our numerical scheme for arc scattering. Since it is very difficult to give an exact solution to this problem with analytic expression, we construct this model with known scattered wave numerically. To this end, the single layer potential is applied.

We construct $u(x)$ by

$$u(x) := \frac{i}{4} \int_{\Gamma} F(\sigma) H_0^{(1)}(k|x-y(\sigma)|) dl_\sigma \quad (4.9)$$

for specified density function $F(\sigma) \in C^2[a, b]$ satisfying $F(x(a)) = F(x(b)) = 0$. Then it can be proven that for $\Gamma \in C^4$ and β_1, β_2 smooth enough, this function generates f_1, f_2 from

$$f_1(\sigma) := \left(\frac{\partial u}{\partial n(x)} + \beta_1 u \right) \Big|_{\Gamma^+}, \quad f_2(\sigma) := \left(\frac{\partial u}{\partial n(x)} - \beta_2 u \right) \Big|_{\Gamma^-}, \quad (4.10)$$

which satisfy the regularity required to apply our numerical method to integral equations (2.14), (2.15). Using (f_1, f_2) , we can solve (μ_{1*}, μ_2) from the system in section 3. Then the numerical result for scattered wave obtained by our scheme is generated from (4.5). Finally we can check the numerical performance by comparing $u(w(t_j))$ obtained in (4.5) with $u(w(t_j))$ computed by (4.9).

To simulate f_1, f_2 from (4.10), we also need to compute the limits of single layer potential as well as normal derivative. This can be done by the standard theory of potential, which

yields

$$\begin{cases} f_1(s) = \frac{1}{2}F(s) + \frac{i}{4} \int_{\Gamma} F(\sigma) \frac{\partial H_0^{(1)}(k|x(s)-y(\sigma)|)}{\partial n(x)} dl_{\sigma} + \beta_1(s) \frac{i}{4} \int_{\Gamma} F(\sigma) H_0^{(1)}(k|x(s)-y(\sigma)|) dl_{\sigma} \\ f_2(s) = -\frac{1}{2}F(s) + \frac{i}{4} \int_{\Gamma} F(\sigma) \frac{\partial H_0^{(1)}(k|x(s)-y(\sigma)|)}{\partial n(x)} dl_{\sigma} - \beta_2(s) \frac{i}{4} \int_{\Gamma} F(\sigma) H_0^{(1)}(k|x(s)-y(\sigma)|) dl_{\sigma} \end{cases}$$

The weakly singular integral can be computed by the previous method.

We present the model problems as follows.

Example 1. We take the wave number as $k = 1.2$ and the arc as

$$\Gamma = \{x : x = (x_1(s), x_2(s)) = 1.4 \times (\cos s, \sin s), s \in [0, \pi/3]\}.$$

The complex impedance on the both sides of Γ is chosen as

$$\beta_1(s) := x_2(s) - i(x_1(s) + x_2(s))^2, \quad \beta_2(s) := -x_1(s) - i(x_1(s) - x_2(s))^2$$

We choose

$$W := \{w := w(t) = (w_1(t), w_2(t)) = 6 \times (\cos t, \sin t) : t \in [0, 2\pi]\}$$

as the points where we compute the scattered wave.

We generate the exact solution by (4.9) with complex density function

$$F(s) = (s - a)(b - s)(x_1(s) + 1 + ix_2(s)). \quad (4.11)$$

Divide the arc Γ by M to solve the density function $(\mu_{1*}(s), \mu_2(s))$ using the boundary values f_1, f_2 simulated above.

The numerics for some special points in W with different M is listed in Table 4.1. The results are very satisfactory, where (E) stands for the exact value, while (N) is the numerically computed values. The exact scattered wave is computed from (4.9) and (4.11), while the numerical results are generated by our scheme. It can be seen that the computation of the scattered wave at the points not near to Γ is very good.

Tab.4.1 Numerics for scattered wave at some points $w(t)$ with different M

t	$M = 32$	$M = 128$	$M = 256$
$0(E)$	(3.8747E-2,2.7374E-2)	(3.8771E-2,2.7394E-2)	(3.8772E-2,2.7395E-2)
$0(N)$	(3.8785E-2,2.7406E-2)	(3.8773E-2,2.7396E-2)	(3.8773E-2,2.7396E-2)
$\frac{\pi}{2}(E)$	(1.1194E-2,4.5476E-2)	(1.1200E-2,4.5513E-2)	(1.1201E-2,4.5515E-2)
$\frac{\pi}{2}(N)$	(1.1204E-2,4.5536E-2)	(1.1201E-2,4.5517E-2)	(1.1201E-2,4.5516E-2)
$\pi(E)$	(-3.9688E-2,-1.2951E-2)	(-3.9725E-2,-1.2958E-2)	(-3.9727E-2,-1.2958E-2)
$\pi(N)$	(-3.9747E-2,-1.2962E-2)	(-3.9729E-2,-1.2959E-2)	(-3.9728E-2,-1.2958E-2)
$\frac{3\pi}{2}(E)$	(-3.8235E-2,8.6009E-3)	(-3.8256E-2,8.6108E-3)	(-3.8257E-2,8.6113E-3)
$\frac{3\pi}{2}(N)$	(-3.8268E-2,8.6168E-3)	(-3.8258E-2,8.6118E-3)	(-3.8257E-2,8.6116E-3)

Tab.4.2 Convergence order for computed scattered wave in W

M	$err(M)$	r
4	2.1334158E-02	–
8	5.2914051E-03	2.0114
16	1.3202773E-03	2.0028
32	3.2991258E-04	2.0007
64	8.2455888E-05	2.0004
128	2.0614320E-05	2.0000
256	5.1686525E-06	1.9958

Now let us check the convergence order of our numerical scheme. Since the exact wave can be computed from (4.9), the convergence order r satisfying $\|u_{num}^M - u_{exa}\| = O(\tau^r)$ with $h = (b - a)/M$ can be computed roughly by

$$r \approx \frac{1}{\ln 2} \ln \frac{\|u_{num}^M - u_{exa}\|}{\|u_{num}^{2M} - u_{exa}\|},$$

where the norm is defined by

$$err(M) := \|u_{num}^M - u_{exa}\|_{L^2} = \left(\frac{\pi}{LL} \sum_{j=0}^{2 \times LL - 1} |u[\mu_1^M, \mu_2^M](w(t_j)) - u(w(t_j))|^2 |\dot{w}(t_j)| \right)^{1/2}$$

to check the convergence order. Here we fixed $LL = 64$. When we compute the density functions for different M , this index r represents the convergence order of the numerical scheme for computing the scattered wave. The results are shown in Table 4.2. Combining Table 4.1 and Table 4.2 together, we can conclude that the numerical scheme is of 2-order convergence with a satisfactory performance.

The far-field can also be checked by comparing (4.8) with the exact value

$$u_{Exact}^\infty(\hat{x}) \approx \frac{e^{i\pi/4}\tau}{\sqrt{8\pi k}} \sum_{l=1}^M F(s_l) e^{-ik\hat{x} \cdot y(s_l)} |\dot{y}(s_l)|, \quad (4.12)$$

noticing that $F(\sigma)$ is smooth and $\mu_2(\sigma)$ is given in $\sigma = s_j$. For $M = 64$ and $LL = 64$, the behavior of exact far-field pattern and the error distribution for the computation of the far-field pattern is shown in Figure 2 and Figure 3, respectively.

Next, we will check the numerics of the scheme for computing the scattered wave near the arc, especially near the tips of the arc.

Example 2. We compute the scattered wave in two parallel surfaces of Γ defined by

$$W^\pm = \{x : x = x_0 \mp n(x_0)\delta, \quad x_0 \in \Gamma\}$$

with the distance $\delta > 0$, where $n(x_0)$ is the normal direction of Γ defined previously, see Figure 4. Notice, M is the number for determining the density functions (μ_1, μ_2) in Γ , while LL determines the number of points where we compute the scattered wave. So we fix $LL = 64, MM = 64$ and consider the numerics for different $\delta > 0$.

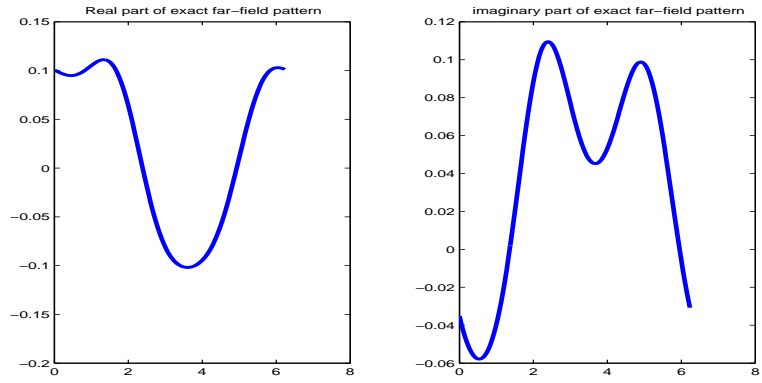


Figure 2: Far-field distribution of real part and imaginary part

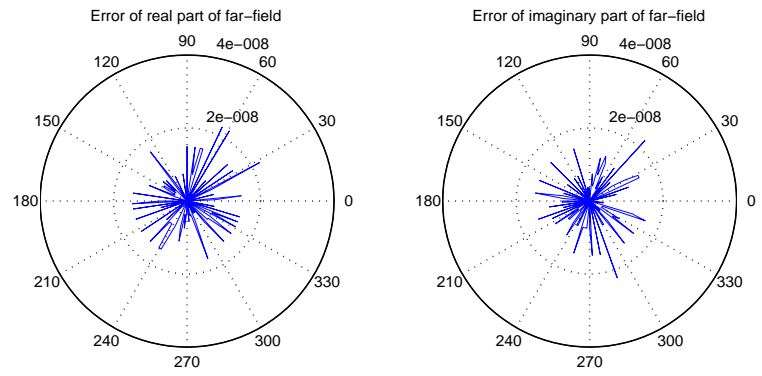


Figure 3: Error distribution of real part and imaginary part

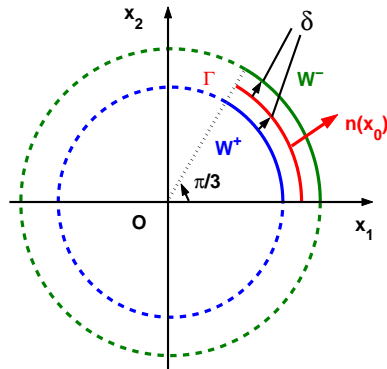


Figure 4: We compute the scattered wave in W^\pm for small $\delta > 0$.

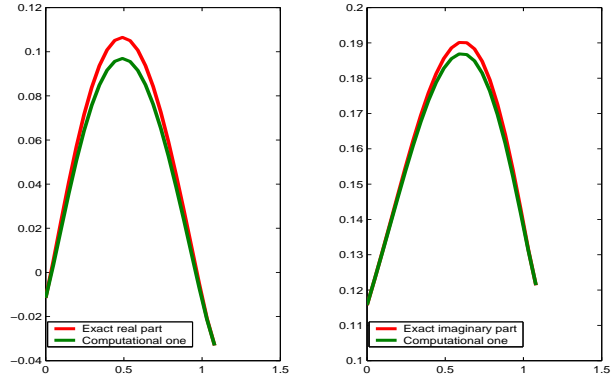


Figure 5: Compute the scattered wave in W^- for $\delta = 0.0001$.

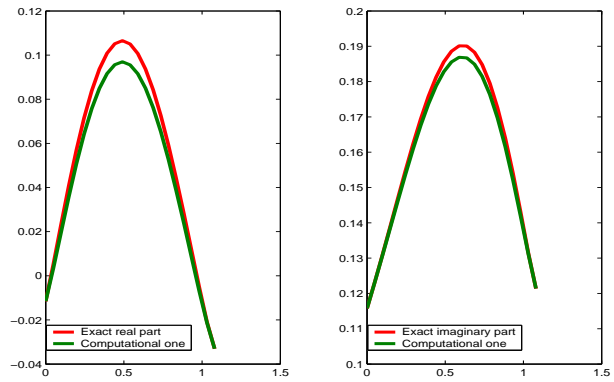


Figure 6: Compute the scattered wave in W^+ for $\delta = 0.0001$.

The results for $M = 64$ with $\delta = 0.0001$ in W^\pm are shown in Figure 5 and Figure 6. It can be seen that the approximation is satisfactory even if for points near to the tips of Γ . Also the continuity of the scattered wave outside Γ is obvious.

To give a quantitative descriptions of the computing scheme near the arc tips, we list the difference $|u_{num}(w^+(t(j))) - u_{exa}(w^+(t(j)))|$ at four points which are near to the two tips of arc. It can be seen from Table 4.3 that the error indeed becomes large for points approaching to the tips of arc.

Tab.4.3 Error of scattered waves in W^+ near to tips for different δ

$t(j)$	$\delta=1\text{E-}3$	$\delta=1\text{E-}4$	$\delta=1\text{E-}5$
$t(1)=4.9067\text{E-}2$	8.2079E-4	1.8052E-3	2.7908E-3
$t(2)=9.8175\text{E-}2$	1.6014E-3	3.4709E-3	5.3479E-3
$t(21)=1.0308$	2.0591E-4	4.9947E-4	7.9552E-4
$t(22)=1.0780$	6.1567E-5	6.1473E-5	6.1569E-5

For the scattering problem of a crack with general shape, it is very difficult to construct the exact solution with analytic expression. So the previous two examples check the performance of the angular potential methods by constructing the exact solution numerically. Now let us consider a straight line segment as the crack with an incident plane wave for which the exact solution can be expressed by the Mathieu functions analytically. For general incident wave, using the superposition principle, the solution for the straight line segment crack can also be constructed theoretically, see [23].

Example 3. Take $\Gamma = \{(x_1, 0) : -h \leq x_1 \leq h\} \subset \mathbb{R}^2$. Consider the following boundary value problem

$$\begin{cases} \Delta u + k^2 u = 0, & x = (x_1, x_2) \in \mathbb{R}^2 \setminus \bar{\Gamma} \\ \frac{\partial u}{\partial n} = -ik \sin \theta \exp(ikx_1 \cos \theta), & x = (x_1, 0) \in \Gamma \\ \frac{\partial u}{\partial |x|} - ik u = o\left(\frac{1}{\sqrt{|x|}}\right), & |x| \rightarrow +\infty, \end{cases} \quad (4.13)$$

where n is directed into $x_2 > 0$ and $\theta \in [0, 2\pi)$ is a given angle. This model can be considered to compute the scattered wave for incident plane wave $u^i(x) = e^{ik(x_1 \cos \theta + x_2 \sin \theta)}$ with Neumann boundary condition $\frac{\partial(u^s + u^i)}{\partial n}|_\Gamma = 0$. Such a configuration is our standard problem (2.2) with

$$\beta_1 \equiv \beta_2 \equiv 0, \quad f_1(x) = f_2(x) = -ik \sin \theta \exp(ikx_1 \cos \theta).$$

Using the standard separation of variable method, the exact solution can be given by

$$u(x, y) = -2\tilde{k} \sum_{n=0}^{\infty} \left[iB_1^{(2n+1)} \frac{Ne_{2n+1}^{(1)}(\xi) se_{2n+1}(\eta) se_{2n+1}(\theta)}{se_{2n+1}(\pi/2)(Ne_{2n+1}^{(1)})'(0)} + \tilde{k}B_2^{(2n+2)} \frac{Ne_{2n+2}^{(1)}(\xi) se_{2n+2}(\eta) se_{2n+2}(\theta)}{se_{2n+2}'(\pi/2)(Ne_{2n+2}^{(1)})'(0)} \right], \quad (4.14)$$

where $\tilde{k} := \frac{kh}{2}$, $(\xi, \eta) \in \mathbb{R}^2$ are the elliptic coordinates satisfying $x_1 + ix_2 = h\text{ch}(\xi + i\eta)$, $se_m(z)$ are the odd periodic Mathieu functions corresponding to $q = \tilde{k}^2$ and $B_m^{(n)}$ are the Fourier coefficients for $se_n(z)$

$$\begin{cases} se_{2n+1}(z) = \sum_{m=0}^{\infty} B_{2m+1}^{(2n+1)} \sin[(2m+1)z], \\ se_{2n+2}(z) = \sum_{m=0}^{\infty} B_{2m+2}^{(2n+2)} \sin[(2m+2)z] \end{cases} \quad (4.15)$$

with the coefficients given by

$$B_{2m+1}^{(2n+1)} = \frac{1}{\pi} \int_0^{2\pi} \sin[(2m+1)z] se_{2n+1}(z) dz, \quad B_{2m+2}^{(2n+2)} = \frac{2}{\pi} \int_0^{\pi} \sin[(2m+2)z] se_{2n+2}(z) dz.$$

$Ne_m^{(1)}(z)$ are the modified Mathieu functions given by the formulas

$$\begin{cases} Ne_{2n+1}^{(1)}(z) = \frac{s_{2n+1}}{B_1^{(2n+1)}} \sum_{r=0}^{\infty} (-1)^r B_{2r+1}^{(2n+1)} [J_r(\tilde{k}e^{-z}) H_{r+1}^{(1)}(\tilde{k}e^z) - J_{r+1}(\tilde{k}e^{-z}) H_r^{(1)}(\tilde{k}e^z)], \\ Ne_{2n+2}^{(1)}(z) = -\frac{s_{2n+2}}{B_2^{(2n+2)}} \sum_{r=0}^{\infty} (-1)^r B_{2r+2}^{(2n+2)} [J_r(\tilde{k}e^{-z}) H_{r+2}^{(1)}(\tilde{k}e^z) - J_{r+2}(\tilde{k}e^{-z}) H_r^{(1)}(\tilde{k}e^z)], \end{cases}$$

where $J_r, H_r^{(1)}$ are the Bessel functions and Hankel the functions, respectively, and

$$s_{2n+1} = \frac{se'_{2n+1}(0) se_{2n+1}(\pi/2)}{\tilde{k} B_1^{(2n+1)}}, \quad s_{2n+2} = \frac{se'_{2n+2}(0) se'_{2n+2}(\pi/2)}{q B_2^{(2n+2)}}.$$

All the values $se'_r(0), se_{2n+1}(\pi/2), se'_{2n+2}(\pi/2), se_r(\theta), se_r(\pi/2), (Ne_r^{(1)})'(0)$ can be computed by the series expression and the limit process. Especially,

$$\begin{cases} (Ne_{2n+1}^{(1)})'(0) = \frac{s_{2n+1}}{B_1^{(2n+1)}} \sum_{r=0}^{\infty} (-1)^r B_{2r+1}^{(2n+1)} \left[H_{r+1}^{(1)}(\tilde{k}) [2\tilde{k} J_{r+1}(\tilde{k}) - (2r+1) J_r(\tilde{k})] + \right. \\ \left. H_r^{(1)}(\tilde{k}) [2\tilde{k} J_r(\tilde{k}) - (2r+1) J_{r+1}(\tilde{k})] \right], \\ (Ne_{2n+2}^{(1)})'(0) = -\frac{s_{2n+2}}{B_2^{(2n+2)}} \sum_{r=0}^{\infty} (-1)^r B_{2r+2}^{(2n+2)} \left[H_{r+2}^{(1)}(\tilde{k}) [\tilde{k} J_{r+1}(\tilde{k}) - 2(r+1) J_r(\tilde{k})] + \right. \\ \left. \tilde{k} H_{r+1}^{(1)}(\tilde{k}) [J_r(\tilde{k}) + J_{r+2}(\tilde{k})] + H_r^{(1)}(\tilde{k}) [\tilde{k} J_{r+1}(\tilde{k}) - 2(r+1) J_{r+2}(\tilde{k})] \right]. \end{cases}$$

Using the above formulas, we can compute the exact solution of (4.13) from the analytic expression (4.14) and then compare the values of u at specified points $w(t_j)$ with those obtained by our angular potential formulas (4.5)-(4.7), where the crack is represented by $\Gamma = \{(x_1(s), x_2(s)) := (-s, 0), s \in [-h, h]\}$ in terms of our parametrization rule. In this way, the proposed numerical scheme by angular potential method can be checked.

Tab.4.4 Numerics for scattered wave at some points of $w_1(t)$

t	$LL = 64$	t	$LL = 64$
$0(E)$	(0.0000,0.0000)	$\pi(E)$	(0.0000,0.0000)
$0(N)$	(-4.6059E-4,5.2675E-4)	$\pi(N)$	(-1.9588E-5,-7.4426E-4)
$\frac{\pi}{4}(E)$	(7.4315E-2,2.9595E-1)	$\frac{5\pi}{4}(E)$	(8.1101E-2,-1.9170E-1)
$\frac{\pi}{4}(N)$	(7.4742E-2,2.9649E-1)	$\frac{5\pi}{4}(N)$	(8.2712E-2,-1.9199E-1)
$\frac{\pi}{2}(E)$	(-4.2074E-2,4.2547E-1)	$\frac{3\pi}{2}(E)$	(4.2074E-2,-4.2547E-1)
$\frac{\pi}{2}(N)$	(-4.2105E-2,4.2509E-1)	$\frac{3\pi}{2}(N)$	(4.3439E-2,-4.2465E-1)
$\frac{3\pi}{4}(E)$	(-8.1101E-2,1.9170E-1)	$\frac{7\pi}{4}(E)$	(-7.4315E-2,-2.9595E-1)
$\frac{3\pi}{4}(N)$	(-8.1836E-2,1.9071E-1)	$\frac{7\pi}{4}(N)$	(-7.4994E-2,-2.9523E-1)

In our model configuration, we compute the scattered wave in two circles $W_i := \{w_i(t) := R_i \times (\cos t, \sin t), t \in [0, 2\pi]\}$ for $R_1 = 6$ and $R_2 = 1.5$. We choose $h = 1$ for the crack and the wave number $k = 2$. The incident wave is specified for $\theta = \frac{\pi}{3}$.

Tab.4.5 Numerics for scattered wave at some points of $w_2(t)$

t	$LL = 64$	t	$LL = 64$
$0(E)$	(0.0000,0.0000)	$\pi(E)$	(0.0000,0.0000)
$0(N)$	(1.1073E-3,-4.5770E-4)	$\pi(N)$	(-6.0305E-4,2.1115E-3)
$\frac{\pi}{4}(E)$	(2.2133E-1,-6.9980E-1)	$\frac{5\pi}{4}(E)$	(-2.5228E-1,2.9074E-1)
$\frac{\pi}{4}(N)$	(2.2177E-1,-7.0146E-1)	$\frac{5\pi}{4}(N)$	(-2.5553E-1,2.8865E-3)
$\frac{\pi}{2}(E)$	(5.2267E-1,-6.1922E-1)	$\frac{3\pi}{2}(E)$	(-5.2267E-1,6.1922E-1)
$\frac{\pi}{2}(N)$	(5.2236E-1,-6.1873E-1)	$\frac{3\pi}{2}(N)$	(-5.2344E-1,6.1639E-1)
$\frac{3\pi}{4}(E)$	(2.5228E-1,-2.9074E-1)	$\frac{7\pi}{4}(E)$	(-2.2133E-1,6.9980E-1)
$\frac{3\pi}{4}(N)$	(2.5213E-1,-2.8792E-1)	$\frac{7\pi}{4}(N)$	(-2.2027E-1,6.9991E-1)

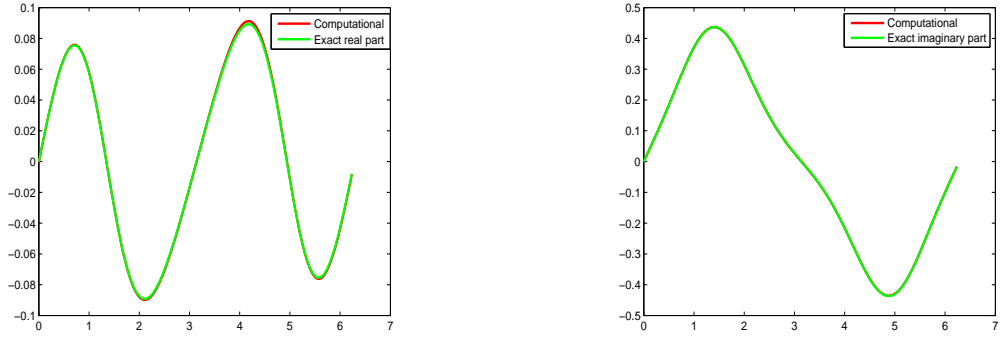


Figure 7: Exact and computed scattered wave in W_1 for straight line segment crack.

In numerical computations, we take $M = 128$ in dividing the crack and truncate the series (4.14) by taking finite summation $\sum_{n=0}^{24}$. The circle $W_i := \{(x_1, x_2) := R_i \times (\cos t, \sin t), t \in [0, 2\pi]\}$ for $i = 1, 2$ is divided as 128 small intervals by taking $t_j = \frac{j\pi}{64}$ with $j = 0, 1, \dots, 127$. The numerical results at some fixed points for the two circles are shown in Table 4.4 and Table 4.5 respectively, while the numerical performance at all points of W_1 is given in Figure 7. Notice, the reconstruction of imaginary part is so well that we cannot distinguish the numerical solution from the exact one in the figure.

From the above three numerical models, we can conclude that the potential method for computing the scattered wave by an open arc is efficient and almost accurate.

Acknowledgement. The work of the first author is supported by NSFC(No.10771033). The first and second authors thank RICAM (Austrian Academy of Sciences) for the hospitality during the special semester on computational biology in 2007 in Linz. The third author

is supported by the Austrian Academy of Sciences via the project SFB F013/1308. The authors also want to thank Prof. Valentina Kolybasova and H.F.Zhao for their contributions in constructing Example 3.

References

- [1] S.M.Belotserkovskii, I.K.Lifanov, Method of Discrete Vortices, CRC Press, Boca Raton, 1993.
- [2] H.Brakhage, P.Werner, Über das Dirichletsche Aussenraumproblem für die Helmholtzsche Schwingungsgleichung, Arch. Math., Vol.16, 325-329, 1965.
- [3] R.Chapko, B.T.Johansson, An alternating potential based approach for a Cauchy problem for the Laplace equation in a planar domain with a cut, Comput. Methods Appl. Math. Vol.8, 315-335, 2008.
- [4] D.Colton, R.Kress, Integral Equation Methods in Scattering theory, John Wiley, New York, 1983.
- [5] D.J.Hoppe, Y.Rahmat-Samii, Impedance Boundary Condition in Electromagnetism, Taylor and Francis, 1995.
- [6] K.D.Ih, D.J.Lee, Development of the direct boundary element method for thin bodies with general boundary condition, J. Sound and Vibration, Vol.202, 361-373, 1997.
- [7] R.Kress, K.M.Lee, Integral equation methods for scattering from an impedance crack, J. Comput. Appl. Maths, Vol.161, No.1, 161-177, 2003.
- [8] R.Kress, P.Serranho, A hybrid method for two-dimensional crack reconstruction, Inverse Problems, Vol.21, 773-784, 2005.
- [9] P.A.Krutitskii, The Helmholtz equation in the exterior of slits in a plane with different impedance boundary conditions on opposite sides of the slits, Quart. Appl. Mathematics, Vol.67, No.1, 73-92, 2009.
- [10] P.A.Krutitskii, D.Y.Kwak, Y.K.Hyon, Numerical treatment of a skew-derivative problem for the Laplace equation in the exterior of an open arc, J. Eng. Math., Vol.59, 25-60, 2007.
- [11] P.A.Krutitskii, Dirichlet's problem for the Helmholtz equation outside cuts in a plane, Computational Math and Mathematical Physics, Vol.34, No.8/9, 1073-1090, 1994.
- [12] P.A.Krutitskii, Neumann's problem for the Helmholtz equation outside cuts in a plane, Computational Math and Mathematical Physics, Vol.34, No.11, 1421-1431, 1994.
- [13] P.A.Krutitskii, Properties of solutions of the Dirichlet problem for the Helmholtz equation in a two-dimensional domain with cuts, Differential Equations, Vol.43, No.9, 1200-1212, 2007.

- [14] P.Krutitskii, J.Liu and M.Sini. Reconstruction of complex cracks by far field measurements, IOP, J. Physics: Conference Series, Vol.135, doi:10.1088/1742-6596/135/1/012056, 2008.
- [15] K.M.Lee, Inverse scattering problem for an impedance crack, Wave Motion, Vol.45, 254-263, 2008.
- [16] K.M.Lee, Inverse scattering via nonlinear integral equations for a Neumann crack, Inverse Problems, Vol.22, 1989-2000, 2006.
- [17] I.K.Lifanov, Singular Integral Equations and Discrete Vortices, VSP, Zeist, 1996.
- [18] I.K.Lifanov, L.N.Poltavskii, G.M.Vainikko, Hypersingular Integral Equations and their Applications, CRC Press, Boca Raton, 2004.
- [19] J.J.Liu, Determination of Dirichlet-to-Neumann map for a mixed boundary problem, Applied Mathematics and Computation, Vol.161, No.3, 843-864, 2005.
- [20] J.J.Liu, G.Nakamura, M.Sini, Reconstruction of the shape and surface impedance from acoustic scattering data for arbitrary cylinder, SIAM J. Applied Mathematics, Vol.67, No.4, 1124-1146, 2007.
- [21] G.Nakamura, M.Sini, Obstacle and boundary determination from scattering data, SIAM J. Math. Anal, Vol.39, No.3, 819-837, 2007.
- [22] O.I.Panich, To a problem on solvability of exterior boundary value problems for wave equation and Maxwell equations, Uspekhi Matematicheskikh Nauk, Vol.20, 221-226, 1965.
- [23] J.J.Stammes, Exact two-dimensional scattering by perfectly reflecting elliptic cylinders, strips and slits, Pure Appl. Opt., Vol.4, 841-855, 1995.
- [24] Y.A.Tuchkin, Wave scattering by an unclosed cylindrical screen of arbitrary profile with the Neumann boundary condition, Soviet Phys. Dokl., Vol.32, No.3, 213-214, 1987.
- [25] H.B.Wang, J.J.Liu, Numerical solution for the Helmholtz equation with mixed boundary condition, Numerical Mathematics A Journal of Chinese Universities, Vol.16, No.3, 203-214, 2007.
- [26] P.Werner, Randwertprobleme der mathematischen Akustik, Arch. Rat. Mech. Anal., Vol.10, 29-66, 1962.
- [27] P.Wolfe, An existence theorem for a reduced wave equation, Proc. Amer. Math Soc., Vol.21, 663-666, 1969.
- [28] Y.V.Zakharov, I.V.Sobynina, One-dimensional integro-differential equations of problems of diffraction by screens, USSR Computational Mathematics and Mathematical Physics, Vol.26, Issue 2, 194-198, 1986.